Results in Engineering 23 (2024) 102306

Contents lists available at ScienceDirect

Results in Engineering

journal homepage: www.sciencedirect.com/journal/results-in-engineering

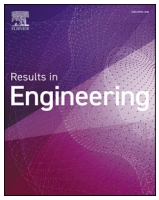

Modeling and simulation of reactors for methanol production by CO_2 reduction: A comparative study

Ramyashree M.S. [a,b], Aparajita Nandy [b], Yash Rameshwar Bohari [a,b], Mahika Pramodh [a,b], S. Harish Kumar [b], S. Shanmuga Priya [a,b,*], K. Sudhakar [c,d,e,**]

[a] VGST Centre of Excellence in Solar Fuels, Department of Chemical Engineering, Manipal Institute of Technology, Manipal Academy of Higher Education, Manipal, 576104, Karnataka, India
[b] Department of Chemical Engineering, Manipal Institute of Technology, Manipal Academy of Higher Education, Manipal, 576104, Karnataka, India
[c] Faculty of Mechanical and Automotive Engineering Technology, Universiti Malaysia, Pahang Al Sultan Abdullah, 26600 Pekan, Pahang, Malaysia
[d] Automotive Engineering Centre, Universiti Malaysia Pahang Al Sultan Abdullah, 26600 Pekan, Pahang, Malaysia
[e] Energy Centre, Maulana Azad National Institute of Technology, Bhopal, 462003, India

ARTICLE INFO

Keywords:
Photocatalysis
Methanol production
CO_2 reduction
Process modelling
Simulation
Reaction mechanism

ABSTRACT

The extensive utilization of fossil fuel energy has caused severe degradation to our environment, therefore the search for new clean efficient energy is the need of the hour. Photocatalytic conversion of CO_2 to solar fuels, and artificial photosynthesis, offer a promising solution for the energy crisis and global warming. Improving efficiency in the photo-reduction of CO_2 to fuels involves developing highly efficient catalysts and optimizing photoreactor configuration. Photocatalysis is a process in which light radiations having energy equal to or greater than the band gap energy (E_{bg}) of a semiconductor strikes on its surface and generates electron (e^-) hole (h^+) pairs. The photogenerated electrons and holes participate in various oxidation and reduction processes to produce final products. This field focuses on harnessing solar energy to drive the conversion of carbon dioxide into hydrocarbon fuels, showcasing significant potential for sustainable energy solutions. The global methanol market was valued at $30.9 billion in 2023 and is projected to reach $38 billion by 2028, growing at 4.2 % CAGR during the forecast period. For determining the feasibility of reactions on a larger scale, simulations must be performed at different conditions for obtaining higher conversion and cost-effective management of the process at the industrial level. So, a simulation of methanol photoreactors using different software was done to examine the kinetics of methanol reactors by employing ASPEN, DWSIM, and MATLAB software for simulating experimental data.

1. Introduction

The ever-increasing requirement for energy has been fuelled by rapid economic growth. A clear result of this is a rise in the use of fuels, especially conventional fossil fuels (coal, oil, and natural gas). The growth in global energy demands has resulted in a significant increase in CO_2 concentration in the atmosphere, as well as global warming. There is a growing interest in capturing CO_2 emissions before they are released into the environment or modifying the fuel to produce positive levels. Photocatalytic hydrogenation is the oldest and most effective approach for converting CO_2 into value-added compounds. Photocatalysts have been studied for their ability to reduce CO_2 and produce various fuel products [1]. Photocatalytic reduction of CO_2 can yield significant chemicals like methane and methanol. Various photocatalysts, such as TiO_2, carbon-based nano-composites, and co-catalysts, have been studied for CO_2 reduction [2]. Carbon capture and removal from industrial sources, as well as reductions in fossil fuel usage, are needed to maintain and potentially reduce average CO_2 concentrations in the atmosphere. Although carbon capture and sequestration have been suggested as solutions, another viable option is carbon capture and recycling, in which CO_2 is recycled into fuels and materials. By combining CO_2 and H_2O several fuel-related products, such as CH_4, CH_3OH, and HCOOH, can be generated. H_2can be made by electrolyzing H_2O with renewable energy

* Corresponding author. VGST Centre of Excellence in Solar Fuels, Department of Chemical Engineering, Manipal Institute of Technology, Manipal Academy of Higher Education, Manipal, 576104, Karnataka, India.
** Corresponding author. Automotive Engineering Centre, Universiti Malaysia Pahang Al Sultan Abdullah, 26600 Pekan, Pahang, Malaysia
E-mail addresses: shan.priya@manipal.edu (S. Shanmuga Priya), sudhakar@umpsa.edu.my (K. Sudhakar).

https://doi.org/10.1016/j.rineng.2024.102306
Received 25 March 2024; Received in revised form 14 May 2024; Accepted 21 May 2024
Available online 25 May 2024

Nomenclature

CO_2 - Carbon dioxide
MOF – Metal organic framework
H_2O - Water
CH_3OH - Methanol
HCOOH – Formic acid
CH_4 - Methane
DMFC - Direct methanol fuel cells
WGS – Water gas shift
DME - Dimethyl ether
H_2 – Hydrogen
OMTP - Offset Multi Tubular Photoreactor
VB – Valence band
CB – Conduction band
DCA - Dichloroacetic Acid
CFD - Computational fluid dynamics
RK - Redlich-Kwong
SRK - Soave-Redlich-Kwong
PR - Peng Robinson
NZCE - Near-zero carbon emission
ODE - Ordinary differential equation
NRTL - Non-random two-liquid
UNIQUAC - Universal quasichemical
RSM - Response surface model
DOE – Design of experiments
CPCP - Compound parabolic collector photoreactor
FPP – Flat plate photoreactor
k – Rate of reaction
K – Equilibrium constant
P – Pressure
T – Temperature
TiO_2 – Titanium oxide
LHHW - Langmuir-Hinshelwood-Hougen-Watson
RSM - Response surface model
SFM - Six-flux model
RTE - Radiative Transfer Equation
DOM - Discrete ordinate method
OVRPA - overall absorption rate of photon absorption
LVRPA - Local volumetric photon absorption rate
VRPA - Volumetric rate of photon absorption
MC - Monte Carlo
LVREA - Local volumetric rate energy absorption

sources, including solar and wind. CO_2 is usually stable and not easily reduced under simple conditions, making traditional methods energy-intensive [3]. There is growing interest in using photocatalysis to turn CO_2 into fuels. This process is more efficient because it uses light energy to activate CO_2 at regular temperatures and lower pressure [4]. Developing a feasible photocatalysis process seems promising in creating energy-rich compounds. The conversion of CO_2 requires activation through the introduction of high-energy electrons. Large-scale CO_2 processes can be energy-intensive, relying on fossil energy and emitting additional CO_2 during combustion.

In the field of photocatalysis, the careful selection of both the photoreactor and catalyst support is crucial for achieving effective photoreduction. An efficient photoreactor is characterized by a high ratio of active catalyst surface area to reactor volume, uniform light distribution and utilization, high photonic efficiency, and high throughput with minimal power consumption [7,8]. Consequently, researchers have dedicated their efforts to exploring methods of anchoring catalysts onto supports to optimize conversion efficiencies. From 1980 to 2000, there was extensive investigation into slurry-type photoreactors for the photocatalytic reduction of CO_2. However, D. Lu et al. studied that the efficiency of CO_2 reduction in a slurry-type reactor faces limitations due to challenges such as uneven light distribution, catalyst attrition, difficulties in product separation, and issues with catalyst recycling [8,9]. Zhou et al. studied that the ultrathin shape of the nanoplates also encourages charge carriers to travel quickly from the interior to the surface to participate in the photoreduction reaction, which should result in better separation of the photogenerated electron and hole and a lower electron-hole recombination rate [3]. Shu et al. studied the development of low-energy CO_2 conversion technologies establishing its importance in decarbonized energy system [10].

As studied by Kothandaraman et al. methanol is the most appealing CO_2 hydrogenation product because it can be used as a drop-in liquid fuel for internal combustion engines and Direct Methanol Fuel Cells (DMFC) [11]. It is one of the most important building blocks in the chemical industry, with an annual production of a billion litre/year. Methanol has a high energy density and can be easily transported and stored, making it a practical option for reducing carbon emissions in transportation. Additionally, the production of methanol from CO_2 helps in recycling and reusing carbon dioxide instead of releasing it into the atmosphere. Its industrial-scale synthesis is based on syngas and $Cu/ZnO/Al_2O_3$-type heterogeneous catalysts under high pressure and high temperature (>200 °C). It has several facets – science, economics, culture, politics, and moral and ethical concerns – and is a global phenomenon that will be felt on local scales for decades and centuries. There is an increasing interest in capturing CO_2 emissions before they are released into the environment, as well as changing fuel to achieve positive amounts. Despite other attempts, photocatalytic hydrogenation remains the oldest and most successful method of turning CO_2 into value-added chemicals. Photocatalysts have been explored for their ability to reduce CO_2 emissions and produce various fuel products [1]. Hossen et al. presented a systematic summary of current advancements and upcoming difficulties in TiO_2-based photocatalysts for CO_2 conversion to hydrocarbon fuels. This review paper thoroughly discusses TiO_2 modification approaches to boost CO_2 photoreduction [12]. Astuti et al. proved the feasibility of an integrated CO_2 capture and utilization system. The study compares the usage of TiO_2 and ZnO photocatalysts for CO_2 reduction to generate formic acid and finds that ZnO is a better photocatalyst than TiO_2 [13].

Hamon et al. stated that Metal Organic Frameworks (MOFs) are gaining popularity as possible co-catalysts for fuel capture and CO_2 conversion. MOFs are well-known for their distinctive properties, including high porosity and chemical tenability [14]. Modified MOF photocatalysts are functionalized to boost light collection while decreasing charge carrier recombination, resulting in increased photocatalytic performance [15]. MOFs offer several advantages for photocatalysis: (1) high porosity facilitates effective exposure of active sites and transport of substrates/products, enhancing catalytic efficiency, (2) tunable structure extends light response range, (3) crystalline nature reduces electron-hole recombination, (4) porous structure shortens charge carrier migration paths, enhancing electron-hole separation, (5) flexible positioning of photosensitizers/cocatalysts promotes spatial separation of electron-hole pairs, and (6) well-defined structures aid in understanding structure-activity relationships. MOFs initiate photocatalytic reactions by harnessing light energy, which excites electrons from the valence band to the conduction band, generating photo-induced charge carriers [16]. Zhang et al. studied several techniques that have been developed to improve the photocatalytic activity of MOFs under solar irradiation, including enriching metal clusters and organic linkers and including foreign photocatalytic species such as metallic debris, semiconductors, and photo sensitizers [17].

These challenges can only be addressed by a mitigation approach. It is by reducing and stabilizing the rate of heat-trapping greenhouse gases in the atmosphere. Earlier, the study of optimization and comparison of reactors for methanol production has not been done so this paper intends to address those gaps.

The objective of the paper is given as follows.

1. To perform ASPEN HYSYS simulation of large-scale methanol production plant for determining the optimum flue gas composition to give maximum conversion into methanol.
2. To conduct kinetic studies for determining the optimum reaction conditions in reactor to get maximum methanol conversion.
3. To perform studies on radiation transport phenomena in various photocatalytic reactor using PHOTOREAC and COMSOL software.

2. Kinetic model for methanol production

2.1. Reaction mechanism

In the present era, methanol is predominantly acquired from syngas through the steam reforming process of natural gas. This comprises four primary stages: feed treatment for desulphurization, reforming to convert methane and steam into syngas, methanol synthesis for the transformation of syngas into methanol and water, and the purification of the final products, concluded by storage [18]. Graaf et al. did a kinetic model study based on dual-site adsorption called as Langmuir-Hinshelwood model using three reactions- Hydrogenation of CO_2, Hydrogenation of CO and RWGS reaction over a commercial Cu/Zn/Al catalyst which are given as Eq (1), Eq (2) and Eq (3) in the paper [19]. After a few years, Bussche et al. studied that only the hydrogenation of CO_2 and WGS reactions together can give the same experimental accuracy [20]. Manenti et al. put forth a dynamic model for a methanol reactor and compared its outcomes with those of a steady-state reactor model, illustrating enhanced stability in the dynamic model [21]. Rahman et al. investigated and validated the kinetic models in the literature by finding the best fit kinetic model developed by varying the CO_2 pressure over Cu-based ZnO/Cr_2O_3 catalysts for methanol formation [22]. Apart from the three governing reactions Lim et al. considered a side reaction from the synthesis of methanol i.e. dimethyl ether (DME). The author includes DME formation since CO_2 shows negative conversions under certain conditions due to reversible water gas shift reaction (WGS). The author explains that for better reduction of CO_2, water production must be increased which can be hence achieved by methanol conversion to DME [23]. Tamnitra et al. group researched bio-methanol formation from biogas. Bio-methanol is also called renewable methanol since it is formed from biogas which is produced from renewables like manure, food, waste, and tapioca starch or sugarcane residue. The two main reactions for methanol production from biogas are methane reforming and methanol synthesis. The methane reforming process consists of three main reactions: dry reforming of methane, steam reforming of methane, and water gas shift reaction. Here, the simulation was done based on the ten thousand litres per day capacity of bio-methanol production. The kinetic model of methanol synthesis is suitable for low-pressure conditions [24]. Azhari et al. evaluated several viewpoints on the catalytic behaviour of several types of catalysts from a mechanistic standpoint, as well as difficulties and insights for future development in terms of the sustainable development of CO_2 hydrogenation to methanol [25]. Bussche et al. devised the model by include the equilibrium term to eliminate the problem of high-pressure circumstances, and it has since been utilized in the majority of the literature [20].

2.2. Methanol reactor simulation

Leonzio et al. derived the findings from an adiabatic kinetic reactor with gas recycle modelled in Aspen Plus, and a methanol reactor with wall heat exchange simulated in MATLAB. Results indicate that, under equilibrium conditions, the reactor with gas recycle achieves the highest CO_2 conversion at 69%, operating at 473 K and 55 bar. Using pure CO_2 and H_2 in the feed results in a lower overall reaction enthalpy change than with syngas. In the MATLAB kinetic simulation of the methanol reactor, minimal axial dispersion was observed, and the impact of the global heat exchange coefficient on reactor performance was less significant than the isothermal heat exchange fluid temperature [26]. Sharifian et al. based their studies on the simulation of CO_2 and CO methanation, using Aspen Plus V8.6. They saw that at a higher pressure, the WGSR has a slight effect on the CO_2 conversion. CO methanation led to more methane as a main product in the outlet stream than CO_2 methanation at the same operating conditions and stoichiometric feed ratio and thus concluded CO methanation is easier than CO_2 at the same conditions [27]. Rujiroj et al. carried out simulation studies of the bio-methanol process from syngas. A one-dimensional heterogeneous model was used to simulate a catalytic reaction in a fixed-bed reactor. The simulation result from the reforming reaction showed an increasing temperature effect on CH_4 and CO_2 conversion, which corresponded to the laboratory findings. Methanol synthesis is best conducted at a temperature of 200 °C and a constant pressure of 4 bar [28]. Nieminen et al. compared the techno-economic potential of a reaction route to methanol via catalytic alcoholic solvents like 2-butanol or 1-butanol and the feasibilities of the conventional gas-phase process employing flowsheet modelling and economic analysis. They found that despite improved methanol yield, the presence of solvent adds complexity to the process and increases separation costs due to the high volatility of the alcohols and the formation of azeotropes. The author concluded that the novel reaction route by providing heat integration could optimize the traditional process. **Eqs (1)–(9)** outlines distinct methodologies for the synthesis of methanol using carbon dioxide and hydrogen [29].

Graaf equation -

$$CO_2 + H_2 \rightarrow CH_3OH \ldots \ldots \ldots. \quad (1)$$

$$CO_2 + 3H_2 \rightarrow CH_3OH + H_2O \ldots \ldots \ldots. \quad (2)$$

$$CO_2 + H_2 \rightarrow CO + H_2O \ldots \ldots \ldots. \quad (3)$$

Vanden et al. equation –

$$CO_2 + 3H_2 \rightarrow CH_3OH + H_2O \ldots \ldots \ldots. \quad (4)$$

$$CO_2 + H_2 \rightarrow CO + H_2O \ldots \ldots \ldots. \quad (5)$$

Lim equation –

$$CO + 2H_2 \rightarrow CH_3OH \ldots \ldots \ldots. \quad (6)$$

$$CO_2 + H_2 \rightarrow CO + H_2O \ldots \ldots \ldots. \quad (7)$$

$$CO_2 + 3H_2 \rightarrow CH_3OH + H_2O \ldots \ldots \ldots. \quad (8)$$

$$2CH_3OH \rightarrow CH_3OCH_3 + H_2O \ldots \ldots \ldots. \quad (9)$$

Kinetic equations of Graaf reactions:

$$R_1 = \frac{k1 * K_{CO}\left[f_{CO} {f_{H_2}}^{1.5} - \frac{f_{CH_3OH}}{{f_{H_2}}^{0.5} * K_1^{eq}}\right]}{\left(1 + K_{CO} * f_{CO} + K_{CO_2}\right)\left[{f_{H_2}}^{0.5} + K_{H_2O} * f_{H_2O}\right]} \quad (10)$$

$$R_2 = \frac{k_2 * K_{CO}\left[f_{CO} {f_{H_2}}^{1.5} - \frac{f_{CH_3OH} f_{H_2O}}{{f_{H_2}}^{0.5} * K_2^{eq}}\right]}{\left(1 + K_{CO} * f_{CO} + K_{CO_2} f_{CO_2}\right)\left[{f_{H_2}}^{0.5} + K_{H_2O} * f_{H_2O}\right]} \quad (11)$$

$$R_{3=} \frac{k_3 K_{CO_2}\left[f_{CO} * f_{H_2} - f_{CO} * \frac{f_{H_2O}}{K_3^{eq}}\right]}{\left(1 + K_{CO} * f_{CO} + K_{CO_2} * f_{CO_2}\right)\left[{f_{H_2}}^{0.5} + K_{H_2O} * f_{H_2O}\right]} \quad (12)$$

Eqs (10)–(12) characterize the kinetics of the three interrelated Graaf reactions required for methanol synthesis.

2.3. Photoreduction mechanism

CO_2 photoreduction comprises complex steps. When considering semiconductor photocatalysts, the semiconductor needs activation through light energy equal to or exceeding its bandgap (E_g), such as light energy ≥3.2 eV for anatase TiO_2. This excitation of the bandgap generates electrons in the conduction band (CB) and holes in the valence band (VB), serving as sites for photoreduction and photooxidation. Additionally, the catalyst must possess electrons with energy surpassing the CO_2 reduction potential [29]. Ali et al. wrote a review on gas-phase photocatalytic CO_2 reduction and studied parameters that influence the actual yield of the photocatalytic CO_2 reduction reactions and outlined the standard testing practices for comparison and evaluation of performance. Moreover, they have calculated the Apparent Quantum Yield (AQY) of different research works, on the basis of data available, for comparing the efficiencies of the photocatalysts [30]. Elhenawy et al. in their review wrote about selective high gas (CO_2) adsorption. The author's concluded for high CO_2 absorption capacity, the temperature must be low since adsorption and temperature follow an exponential graph [31].

2.4. Review of simulation carried in PHOTOCATALYTIC reactor

The complexity resulting from photochemical reactions and radiation transport poses a challenge. Nonetheless, employing photoreactor models is essential for simplifying experiments and conducting thorough result analyses. Herazo et al. formed an open-access application developed in the graphical user interface of MATLAB named PHOTOREAC. The application was modelled to study solar photoreactor configurations and kinetic studies related to solar degradation of water contaminants. They performed solar photodegradation of Dichloroacetic Acid (DCA) and methylene blue in CPCP and OMTP reactors using TiO_2 P25 Evonik as photocatalyst with a radiation field study of a Flat Plate Photoreactor (FPP). Because of the fitted reflectors, the author concluded that the CPCP can absorb more solar radiation per length than the OMTP reactors with less volume [32].

Pareek et al. conducted experiment on photodegradation of spent bayer liquor in an 18-L pilot-scale photoreactor with a UV lamp source of range (250–400 nm). The Eulerian multiphase model was simulated in FLUENT 6.0 (CFD) which also simulated RTE (Radiation Transport Equation) [33,34]. Grzywacz et al. presents a model of a flat plate photocatalytic reactor under solar radiation. Convection and diffusive mass flux balances in two zones were used to build the model: a thin liquid layer and pores in a porous catalyst layer. The flux of light intensity was described by Kubelka–Munk theory. Light penetrating an endless plate on both sides, according to the Kubelka–Munk theory, changes due to light absorption or scattering on penetrated media [35]. Janczarek et al. presented a review of computer simulations of photocatalytic reactors discussing different model methods helpful for scaling photocatalytic reactors like the Monte Carlo method, approximation approach–P1 model, and CFD (Computational Fluid Dynamics) as a simulation tool [36]. Marečic et al. work dealt with the photocatalytic oxidation of toluene at room temperature and atmospheric pressure in the gas phase. The reaction was performed in an annular reactor using a UVA black light blue fluorescent lamp. The behaviour of a photocatalytic annular reactor with titanium dioxide as the oxidation catalyst was simulated using various mathematical models, including 1D and 2D heterogeneous models based on ideal flow and laminar flow conditions. With 2D heterogeneous models, better estimation results are obtained when the root mean square deviation is used as a correlation criterion [37]. Ye et al. has explained 3D & 2D enthalpy-porosity by simulating pure solid-gallium [38]. Author explores the relationship between the mushy zone constant (Am) and the driving temperature difference (ΔT) during the melting of calcium chloride hexahydrate [39]. False diffusion mechanisms, asymmetrical interface phenomena, and equilibrium state results of pure gallium melting in the perfectly symmetric rectangular-enclosure are successively explored and comprehensively discussed by the author [40]. The revised definition and proven computational method of the interface error between numerical and experimental results are presented in detail, thereafter, the 2D verification and 2D validation of enthalpy-porosity modelling of melting process of gallium in a rectangular enclosure heated from a vertical wall [41].

Moreno et al. researched to improve the numerical simulation of the radiation field in three different types of photoreactors i.e.an annular reactor lit up by a mercury UV-A lamp radiating isotropic emission, a tubular reactor with a compound parabolic solar collector radiating parallel emission and a tubular reactor radiating cone-shaped and power-cosine emissions. The simulations were compared between ANSYS Fluent and Open FOAM software. The results were validated and hence was concluded that CFD is a very powerful and reliable tool for the simulation of photoactivated processes [42]. Topare et al. conducted a thermal analysis of a photocatalytic reactor made of glass was carried out in SolidWorks software. Reactor operating conditions ranged from 25°C to 80°C and 1 atm. pressure. The photocatalytic reactor concentrated on the degradation of organic pollutants in water [43]. Wang et al. studied the influence of multiphase flow on the radiation dispersion in a slurry reactor in a quantitative manner. In the photocatalytic slurry reactor water, air, and catalyst particles exist together making it a multiphase reactor. They studied the radiation effects in a multiphase slurry reactor and discovered that non-uniformity of flow [44].

Gai et al. gives a detailed description of Near-Zero Carbon Emission (NZCE) powerplant. The author talks in-depth about the mitigation of CO_2 using various techniques such as electrolysis cells, F-T reactor, and electrocatalytic reactor conversion of CO_2 and H_2O to liquid fuel. The author makes use of ASPEN software for carrying out simulation studies. The author presents a comprehensive study of different routes for carrying out liquid fuel generation using CO_2 along with flowsheets. The different routes that the author takes are the synthesis of methanol using CO + H_2, and methanol synthesis using CO_2+H_2 and CO_2+H_2O. The author compares the results obtained by these three methods and conducted an economic analysis of the NZCE powerplant [45]. Ghasemian et al. studied the solubility of CO_2 in water at 278.15K–348.15K and 0.1–1 MPa. The author compares the experimental data with those obtained from different equations of state such as van der Waals, RK, SRK, and PR. The author also models the solubility of carbon dioxide in water using Artificial neural networks and optimizes using the Genetic Algorithm method. The author discusses the results obtained from these methods [46]. Salvi et al. talks about various carbon separation and carbon capture techniques including absorption into liquid, gas phase separation, and adsorption on solid and hybrid processes such as adsorption-membrane systems. Furthermore, the regulations for CCS, economic research, and strategy concerns have also been discussed [47]. López et al. give a review of the recent advances in the development of heterogeneous catalysts and the process for direct hydrogenation of CO_2 to methanol. The author focuses on the improvement of conventional Cu/ZnO-based catalysts and the development of a new catalytic system targeting the specific needs for CO_2 to methanol reactions. The author also summarizes future research and development perspectives on effective heterogeneous catalysts for methanol synthesis from CO_2 [48].

Scientists use photoreactor models to unravel the complexities of photochemical reactions. Researchers have explored solar photoreactors, employing simulations with tools such as FLUENT and SolidWorks for enhanced understanding. Advancements in heterogeneous catalysts for converting CO_2 to methanol and investigations into carbon separation techniques contribute to the progress of sustainable energy and environmental studies. After completing a literature review on the topics of methanol reaction mechanism and simulation; photocatalytic reaction mechanism and its simulations many conclusions can be reached. Authors have used different catalysts like Cu/ZnO and MOFs. The results have been validated by different software like design-expert etc. There has been research on radiation and hydrodynamic studies of different reactors like annular, batch, continuous flow reactors, etc. with simulation studies in CFD, COMSOL, etc [49].

3. Methodology for conducting simulation

The method for conducting reactor kinetic and radiation effects simulations is described in detail. For simulations, we use different software segregated according to their usage, complexities, special solver features, etc. All flowsheet simulations: ASPEN, DWSIM, work under underlying relationships mass balance, equilibrium relationships, compositions, enthalpy balance, and rate correlations. These predict output flow rate, compositions, feasibility of process under specific operating conditions, equipment sizing, etc. Aspen Plus, DWSIM, etc. are used as a process flowsheet simulator in major chemical industries. They are used in real-world applications from interpreting laboratory-scale data to full-scale plants. Table 1 illustrates the advantages and limitations of different softwares.

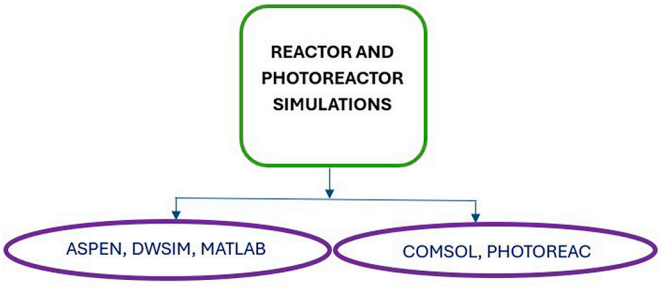

3.1. Reactor model studies

3.1.1. ASPEN plus

Aspen Plus is the oldest method used by chemical engineers for developing flowsheets. Aspen Plus, initially designed as a sequential modular simulator, has evolved to include advanced features. It can now integrate with specialized software for tasks like detailed heat exchanger design, dynamic simulation, batch process modelling, cost estimation, and more. Additionally, Aspen Plus provides users with the option to apply an equation-based approach to its functions [50]. Aspen Plus is used to perform mainly 6-unit operations namely Mixers/Splitters, Separators, Exchangers, Columns, Reactors, and Pressure Changers used for specific purposes in chemical Industries. In this work, we study the methanol conversion in different reactors which can be solved by in-built reactor models namely RSTOIC, RYIELD, REQUIL, RGIBBS, RPLUG, RCSTR, and RBATCH. RSTOIC is used in cases where only stoichiometry is known not the reaction mechanism. When both the reaction kinetics and stoichiometry are unknown RYIELD is used for single-phase chemical equilibrium or simultaneous-phase equilibrium calculations. RBATCH, RPLUG, and RCSTR come under rigorous models since they incorporate built-in power law, Langmuir-Hinshel wood-Hougen-Watson (LHHW) kinetics, or other kinetics specified by the user. In this work, a batch reactor has been chosen which can be replicated in lab-scale methanol generation. An isothermal batch reactor with inlet feed temperature, and pressure as 40 degrees C and 1 atm respectively with reactor temperature, and pressure specified as 543k and 10 MPa resp.

3.1.1.1. Theory. The processing of methanol is an overall exothermic process that employs a strong catalyst [48]. The rate is in general described by a power law or Langmuir-Hinshelwood reactions.

$$R = \frac{(\text{kinetic factor})(\text{driving force expression})}{(\text{adsorption term})} \tag{13}$$

This is the LHHW kinetic expression used in ASPEN PLUS. The LHHW kinetic model is made up of a kinetic factor (in the simplest cases, equal to the kinetic constant, but more generally dependent on it), a driving force expression (depending on the reactants available in the reaction medium), and an adsorption term, which weights the reactants truly available on the catalyst surface, which may be much lower than those present in the gas/liquid phase [51]. The equations of Vanden are used in this work: **Eq (14)** gives the rate of the first reaction to produce methanol from carbon dioxide, while **Eq (15)** gives the rate of the water-shift reaction.

$$R_1 = (k_4 P_{CO2} P_{H2}) \frac{\left[1 - \frac{1}{KE1}(PCH3OH * PH2O)\right]}{[1 + k3\left(\frac{PH2o}{PH2}\right) + k1\sqrt{PH2} + k2PH2O\widehat{]}3} \tag{14}$$

$$R_2 = (k_5 P_{CO2}) \frac{\left[1 - \frac{1}{KE2}\left(\frac{PCO * PH2O}{PCO2 * PH2}\right)\right]}{[1 + K3\left(\frac{PH2O}{PH2}\right) + K1\sqrt{PH2} + K3PH2O]} \tag{15}$$

All the kinetic coefficients of the equations that are stated in further equations for use in the Aspen–Plus form were explained [52]. These are mentioned in **Eq 16** and **Eq 17**.

$$R_{CH_3OH}(\text{kmol/kg.s}) = \frac{\left(1.07*10^{-13}*e^{\left(\frac{4413.76}{T}\right)}*P_{CO_2}*P_{H_2} - 4.182*10^{7}*e^{\left(\frac{-2645.966}{T}\right)}*\frac{P_{CH_3OH}*P_{H_2O}}{P_{H_2}^{\,2}}\right)}{\left(1 + 3453.38*\left(\frac{P_{H2O}}{P_{H2}}\right) + 1.578*10^{-3}*P_{H_2}^{\,0.5} + 6.62*10^{-16}*e^{\frac{14928.915}{T}}*P_{H_2O}\,\widehat{)}3\right)} \tag{16}$$

$$R_{CO}(\text{kmol/kgcat.s}) \frac{122*e^{-\left(\frac{11398.244}{T}\right)}\left(P_{CO_2} - 0.009354*e^{\frac{4773.259}{T}}*\frac{P_{CO}*P_{H2O}}{P_{H_2}}\right)}{\left(1 + 3453.38*\frac{P_{H_2O}}{P_{H_2}} + 1.578*10^{-3}*e^{\frac{2068.44}{T}}*P_{H_2}{}^{5} + 6.62*10^{-16}*e^{\frac{14928.915}{T}}*P_{H_2O}\right)} \tag{17}$$

The available number of reactants in the fluid phase, each with its reaction order, is represented by the 'driving force' component, which considers forward and potential reverse reactions (the latter with a negative sign). It takes the following form where K_1 and K_2 are equilibrium constants, and K_1 is often set to 1. The driving force is represented in **Eq (18)**.

$$\text{Driving Force} = k_1 \Pi C_i^{\alpha} - k_2 \Pi C_i^{\beta} \tag{18}$$

$$\text{Adsorption} = \{1 + k_w[W] + k_x[X] + k_y[Y] + k_2[Z]\}\hat{n} \tag{19}$$

In LHHW reactions, the “Adsorption Expression" is determined by the presumed adsorption process. Expressions are found in Ref. [53].

Since methanol is formed at a pressure greater than 10 bar, it is recommended that we use an equation of state, such as “SR-POLAR," “SRK," or “PSRK," in the Property Method Selection Assistant. SRK method was chosen as an equation of state.

$$\ln(k_f) = A + B/T + C\ln(T) + DT \quad (20)$$

- “Term 1” is mentioned for forward reaction as

$$A + (B/T) = \ln(1.07 \times 10 - 13 \times e(4413.76/T))$$

$$A = -29.866;\ B = 4413.76$$

- “Term 2” is mentioned for backward reaction as

$$A + (B/T) = \ln(4.182 \times 107 \times e(-2645.966/T)$$

$$A = 17.5489;\ B = -2645.97$$

Values given in **Eq (16)**.

Similarly, the Next reaction is mentioned by following the same steps mentioned above. Here, the reaction goes $CO_2 + H_2 \rightarrow H_2O + CO$.

3.1.1.2. Procedure.

3.1.1.3. Process description-. The process was simulated in Aspen HYSYS software [50].

- Feed inlets containing flue gases like H_2, N_2, CO, CO_2, CH_4, and H_2O were considered to have compositions of 0.6760, 0.0032, 0.0380, 0.2569, 0.0234, 0.0025, etc. The inlet feed (stream 1) was given at a temperature and pressure of 50 °C and 51.2 bar, respectively.
- The inlet feed was further compressed and thus compressed feed 2 attained a temperature and pressure of 95.65 °C and 75 bar, respectively.
- The compressed feed was cooled to 60 °C (stream 3) which was further compressed (stream 4) and thus the stream temperature and pressure rose to 107 °C and 110 bar. The feed is added to a mixer, mixed with a recycle stream from recycle unit 2 (5), and sent to another mixture unit further mixed with a stream coming from recycle unit 1.
- The outlet (stream 6) from the mixture is added to a 1,2-pass counter-current heat exchanger where the stream gets heated to 145 °C from a stream coming from the reactor thus integrating heat in the process of forming a high amount of methanol. Two streams coming from the shell and tube side of the heat exchanger are sent to coolers and heaters, respectively.
- The tube side stream is heated from 145 °C to 150 °C (stream 8) to attain the reactor conditions for the specified reactions to take place. Reactions taking place are:

$$CO + 2H_2 \rightarrow CH_3OH \quad (21)$$

$$CO_2 + 3H_2 \rightarrow CH_3OH + H_2O \quad (22)$$

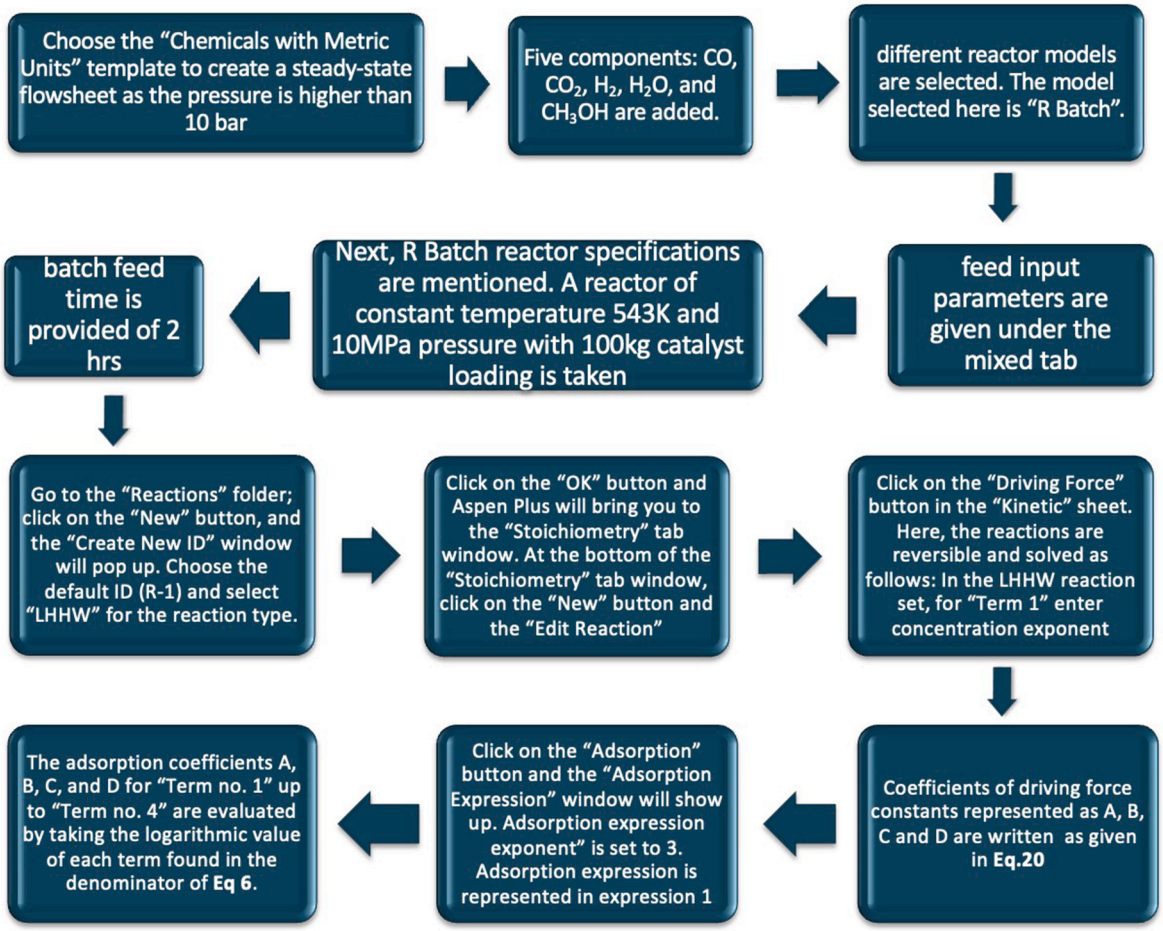

Table 1
The advantages and limitations of different simulation methodologies.

	ADVANTAGES	LIMITATIONS
ASPEN HYSYS	1. Its flexibility, accuracy, and strength help create more realistic models and can be used in different areas, including gas production [65]. 2. It is a commercially established software widely utilized in the process industry for its capabilities in simulating both steady-state and dynamic processes. 3. Simplifying the process by removing obstacles and reducing the intricacies in the process network. Enhances control and operability of the plant [65].	1. A major limitation discovered was the incapability of transferring vectors from HYSYS back to Unity. 2. Aspen HYSYS does not include membranes as part of its standard set of process functions [66].
PHOTOREAC	1. The PHOTOREAC software was utilized to assess photon absorption (OVRPA) in the photocatalytic process and to simulate photocatalytic reactions using the available kinetic model database [67] 2. It offers four kinetic models that can best fit the reaction kinetics data, namely Langmuir-Hinshelwood, Zalazar, Ballari, and Mueses's kinetic models [67]	The PHOTOREAC software relies on a set of assumptions to address the differential equations and extract the kinetic parameters. These assumptions involve: • The absence of limitations in mass transfer. • Treating convection and diffusion as a centralized system. • Assuming differential conversion per pass [65].
DWSIM	1. It is an open-source application, is freely available, and provides capabilities for both steady-state and dynamic simulations. 2. DWSIM, being an open-source application, is freely available and provides capabilities for both steady-state and dynamic simulations. 3. It features an interface that is easy to use. As an example, Jonach et al. utilized DWSIM to model and simulate 3-phase separators within the oil and gas industry [67, 68].	1. Less widely adopted in the industry compared to commercial tools. 2. The execution process of the simulation is time-consuming.
COMSOL **MULTIPHYSICS**	1. It is applicable in diverse fields such as heat exchangers, cutting tools, solar and energy systems, and optical and manufacturing processes [69]. 2. It is unique due to its ability to handle complex shapes and various physical phenomena.	1. Certain simulations might require a substantial number of computational resources. 2. The software is expensive, especially for students and individual researchers, with a base license costing $4000.

- The shell side stream goes to a cooler and gets cooled from 175 °C to 38 °C (stream 12).
- The cooled stream goes to the separator (V-100) where it gets separated into vapor and liquid phases. The vapor stream (stream 13) is split and sent to the compressor (K-102), after being compressed it is further mixed with the liquid stream (stream 25), which is separated in a separator (V-101) (stream 23) and compressed (K-103) (stream 25) before going to the mixer.
- The mixed stream (stream 18) is again recycled (stream19) which is added back to the mixture unit (MIX-101).
- The liquid stream from the separator (V-101) (stream 24) goes to the distillation column (T-100)

3.1.2. *MATLAB*

MATLAB proves valuable in simulating photoreactors, offering researchers an accessible and adaptable means to model and comprehend intricate processes, particularly in photoreactors, where accurate simulation of light-driven chemical reactions is essential. Executing methanol synthesis simulations in MATLAB requires developing a computational model that accurately depicts the chemical reactions and processes intrinsic to the synthesis. In the selection of a solver for the system's differential equations, one can opt for a suitable option like MATLAB's ODE solvers, such as ode45, renowned for their proficiency in handling ordinary differential equations. Application of numerical methods is done to effectively address and resolve the system of equations. The Ordinary Differential Equation (ODE) solvers in MATLAB solve initial value problems with a variety of properties. The solvers can work on stiff or non-stiff problems, problems with a mass matrix, Differential Algebraic Equations (DAEs), or fully implicit problems. The MATLAB and Simulink functions: ode23 and ode45 are the primary methods for solving non-stiff ordinary differential equations. The Runge-Kutta method ode23 is a three-stage, third-order Runge-Kutta method. The Runge-Kutta method ode45 is a six-stage, fifth-order Runge-Kutta method. While ode45 performs more work per step than ode23, it can take far larger steps. Ode45 is also more accurate than ode23 for differential equations with smooth solutions.

3.1.3. *DWSIM*

DWSIM, developed by Daniel Medeiros, is a no-cost chemical process simulation tool for understanding chemical processes. It is freely accessible as an open-source platform, allowing users to explore the behavior of chemical systems without any charges [54]. DWSIM, recognized as a free alternative, is suggested for its potential to perform at a level comparable to commercial software. It has been employed in various applications, including analyzing and simulating biodiesel production, conducting techno-economic studies on biorefineries, and investigating energy generation possibilities from solid biomass [55]. It allows one to conduct experiments and analyze data using advanced models and operations. It is used to evaluate material conversion efficiency and determine optimal energy needs in processes with light elements C and H, vital for creating low or zero-emission fuels from hydrocarbons. Its flexibility allows focused analyses on components like reactors or entire facilities, exploring various scenarios for economic assessments while maintaining originality [56]. It has built-in thermodynamic models and unit operations as well as a large range of tools for managing reactions or creating components. Some popular property packages are also available, such as Peng-Robinson, NRTL, UNIQUAC, Raoult's Law, Lee-Kesler, etc. Utilization of visualization tools in DWSIM is done to create graphical representations, including plots and charts, that depict changes in concentration, temperature profiles, and other relevant data.

3.1.3.1. Process description. Feed inlets and reactor configurations were taken from Froment et al. [15].

Feed conditions were as follows:
Catalyst Density (kg/m^{3}s) = 1775;
Porosity = 0.5;
Mass (g) = 34.8;
Pellet diameter(m) = 0.0005;

Reactor: Diameter(m) = 0.016; Length(m) = 0.15;

Operating conditions: T(K) = 493.2,P(bar) = 50,m(10ˆ(−5)kg/s) = 2.8; Feed composition- CO (mol%):4.00, H_2 (mol%):82.00, CO_2 (mol %):3.00, Inert (mol%):11.

3.1.4. *Design expert*

Design-Expert serves as a statistical software, differing from process simulation tools like DWSIM. Its utility lies in designing experiments (DOE) and performing statistical analyses to improve the optimization of methanol synthesis processes. Comparative tests, screening, characterization, optimization, robust parameter design, mixture designs, and mixed designs are all available via Design–Expert. Design expert offers

test matrices for screening up to 50 factors. Analysis of variance is used to assess the statistical significance of these variables (ANOVA). Graphical tools aid in determining the effect of each factor on the desired outcomes and revealing hidden information. By varying the values of all factors in parallel, the program calculates the key effects of each factor as well as the interactions between them. With a small number of experiments, a Response Surface Model (RSM) can be used to map out a design space. By varying the values of all factors, RSM provides an approximation for the importance of responses for any possible combination of the factors. A study was conducted improve methanol production from a methanol reactor by employing Design of Experiments (DOE) with Design Expert, while utilizing Aspen Plus as a reactor simulator. The optimization process encompasses eight parameters, including five inlet molar flowrates (CO, CO_2, H_2O, H_2, CH_3OH) and three reactor conditions (inlet temperature, pressure, and temperature profile). In Design Expert, the optimization of methanol production utilized the Box-Behnken method along with a quadratic model [57].

3.2. PHOTOCATALYTIC reactor studies

Heterogeneous photocatalysis is a photochemical reaction in which a light-absorbing catalyst, referred to as a photocatalyst, improves the rate of the reaction by providing a more energy-efficient reaction route. A photocatalytic reaction begins when photons with ample energy-energy greater than the photocatalyst's band gap are absorbed by the photocatalyst and excite the electrons into the conduction band which leaves positive holes in the valence band of the photocatalyst [58]. The most used materials are doped TiO_2, perovskites, MOFs, g-C_3N_4, etc. which show high efficiency in the optical medium due to characteristics like band gap, charge separation, and charge transfer. TiO_2 is widely recognized as a versatile semiconductor for treating wastewater, thanks to its strong ability to use light for chemical reactions, stability in different environments, and corrosion resistance [59]. The rate of photoreaction depends on the number of photons absorbed by the photocatalyst. In a photoreactor, intensity decays due to absorption a scattering phenomenon of the photocatalysts located at different places in the reactor, also depending on reactor volume and geometry. The creation of mathematical models such as the radiation absorption-scattering model, the radiation emission model, the kinetic model, and the fluid-dynamic model are all needed for this process. These are complex numerical systems consisting of differential equations. Static collectors with an involute reflective surface encircling a cylindrical reactor tube are known as CPCs. They've been discovered to have the best optics for systems with low solar radiation concentrations, and they can be equipped with a focusing ratio close to one to absorb both direct and diffuse UV sunlight. Almost all of the UV radiation that reaches the CPC aperture can be reflected. The tubular reactor combined with a Compound Parabolic Collector (CPC) has been proposed to be a potential choice for large-scale photocatalytic hydrogen production. The efficiency of these collectors lies between 50% and 70 % [60]. Designing a photocatalytic reactor for environmental applications in heterogeneous photocatalysis is challenging due to the distinct phases of the three involved components: pollutants in fluid, catalyst in a solid state, and light photons as massless particles. The heterogeneous nature of photocatalysis adds complexity to reactor design, requiring interdisciplinary expertise spanning chemical, mechanical, and environmental engineering concepts [61].

3.2.1. Radiative models

Radiative models are the crucial and most important part of photocatalytic study which help in calculating the rate of photon absorption and thus deciding the kinetic of photoreaction. LVREA is evaluated by solving the Radiation Rransfer Equation (RTE) given Eq (23).

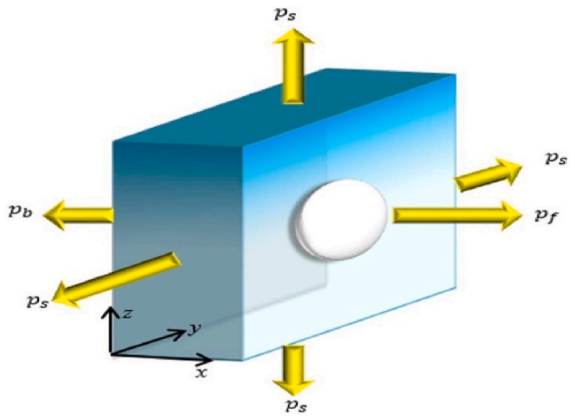

Fig. 1. The six principal directions of photon scattering in the six-flux model (SFM) and the scattering probabilities [5].

$$dI_\lambda(x,\Omega)/dx = -\beta_\lambda I_\lambda(x,\Omega) + \sigma_\lambda/2\int_{4\pi} I_\lambda(x,\Omega)p(\Omega\rightarrow\Omega')\,d\Omega \quad (23)$$

The key modelling approach uses the Discrete Ordination Method (DOM) suggested by Duderstadt and Martin to solve the RTE rigorously. In heterogeneous photocatalytic systems, the RTE solved by the DOM method allows for an accurate prediction of the radiation fields. Based on the solution of Mie's theoretical equation, this method has been validated with simulation results [62]. There are specific limitations of this method hindering them at the solar scale. Under a variable solar flux, the computational demand of the RTE-DOM becomes quite prohibitive.

SFM (Six-flux model): The model has many assumptions as follows.

i. Large-spaced particles.
ii. Particles are distributed uniformly across the space considered.
iii. The fluid is transparent to UV irradiation.
iv. The heterogeneous system emits no light.
v. Only scattering or absorption occurs When a photon strikes a particle.
vi. The scattering can only occur along six directions of the Cartesian coordinates as shown.

A new simple model was devised, where photons are supposed to be scattered in any of the six principal directions concerning the incoming radiation as shown in Fig. 1. Six different photon fluxes must be considered in this case, hence the name Six-Flux Model (SFM) [63].

DOM (Discrete Ordinate Method):

Analyzing radiative heat transfer is complex and costly. Recent efforts aim to enhance approximate methods. Method efficiency depends on the quadrature schemes for computing source terms and heat flux. The Discrete Ordinate Method (DOM) is one of the earliest and most widely used, with proposed schemes to improve its computational appeal over time [64]. The incident radiation in the DOM is measured by integrating the radiant intensity along spherical space directions. The method begins by discretizing spatial directions (quadrature) and then solving the Radiative Transfer Equation (RTE) in each of them. The effect of light absorption and dispersion is included in the RTE. The incident radiation on a given point within the reaction space was evaluated using FFM in this project. The total radiation flux is calculated in this model as the number of photon fluxes travelling from the light source to that point and photon fluxes from scattering in both axial and

radial directions. The incident radiation flux (gf), the backscattering flux (GB), and the fluxes entering the differential portion from the bottom and upper walls ((ga) and (gc)) are the four fluxes that this model accounts for as shown in Fig. 2. Back-scattering probabilities in the corresponding directions are expressed by the parameters pf, pb, pa, and pc.

The LVREA using the four-flux model is given in Eq (24):

$$\mathrm{LVREA} = g_{\mathrm{total}}\, k_{\lambda} \;/\; V * \left(R_{\mathrm{lamp}}\, \delta \;/\; 4r^{2}\right) \tag{24}$$

PHOTOCATALYTIC KINETICS is given in Eq (25):

$$r = k1 f(C) g(Ea) \tag{25}$$

where f(C) part describes the rate dependency on concentration and g (E_a) indicates the rate of photon absorption.

3.2.2. COMSOL Multiphysics software

There are various CFD simulation frameworks available. Some of them are commercial, such as ANSYS Fluent and COMSOL Multiphysics, and others are open-source CFD software, e.g., Open-FOAM and FEATFLOW. To make the modelling process easier, the following assumptions were made.

1. The reaction takes place at a steady temperature of 35 °C.
2. The photocatalyst particles, bubbles, and water are homogeneous, and light radiates evenly through the photocatalyst surfaces.
3. Turbulent flow dominates at all reaction sites.
4. The photocatalytic reaction takes place only at the surfactant stage.

Modules used by COMSOL Multiphysics are the Heat transfer module, Euler–Euler, Turbulent model k-Ɛ and Transport of Diluted Species.

3.2.2.1. Procedure

$$\mathrm{IRintz} = S1 \;/\; 4\pi \mathrm{Rint} * [a\tan((2z - \mathrm{LR} + \mathrm{Llamp}) \;/\; 2\mathrm{Rint}) - a\tan((2z - \mathrm{LR} - \mathrm{Llamp}) \;/\; 2\mathrm{Rint}) \tag{26}$$

where S1 = 2π*radius lamp* Iw.

3.2.3. PHOTOREAC

PHOTOSTREAM is a user-friendly MATLAB tool for evaluating solar photoreactor performance. It includes various reactor setups, reaction models, and radiation absorption-scattering approaches. The tool has a dataset of 26 experiments on solar degradation, covering different conditions like pollutant types and initial levels. Users can easily add their experimental data [26]. It is based on the results of study groups at Cartagena University (Cartagena de Indias, Colombia) and Universidad del Valle (Valle del Valle, Colombia) (Cali, Colombia) in the last 20 years of extensive research on solar photocatalysis. Users will be able to investigate the impact of critical device parameters on the photoreactor's radiation absorption efficiency and the overall kinetic activity of the photocatalytic mechanism by using PHOTOREAC. It provides an interface that users can readily use. Users will be able to investigate the impact of critical device parameters on the photoreactor's radiation absorption efficiency and the overall kinetic activity of the photocatalytic mechanism by using PHOTOREAC. Herazo et al. performed the simulations with the PHOTOREAC environment, which includes three configurations of pilot-scale solar photoreactors: a flat plate photoreactor (FPP), a compound Parabolic Collector Photoreactor (CPCP), and the Offset Multi-Tubular Photoreactor (OMTP). For the TTP, a novel prototype is also included, the OMTP. The photoreactor is exposed to the sunlight, facing the sun, while the reservoir tank is in the dark. The photon absorption-scattering model provides the LVRPA spatial distribution inside the photoreactor called as local volumetric rate of photon adsorption. The six-flux absorption-scattering model is the subject of the PHOTOREAC modelling. SFM is an empirical equation based on the hypothesis that scattering exists only in the six Cartesian directions.

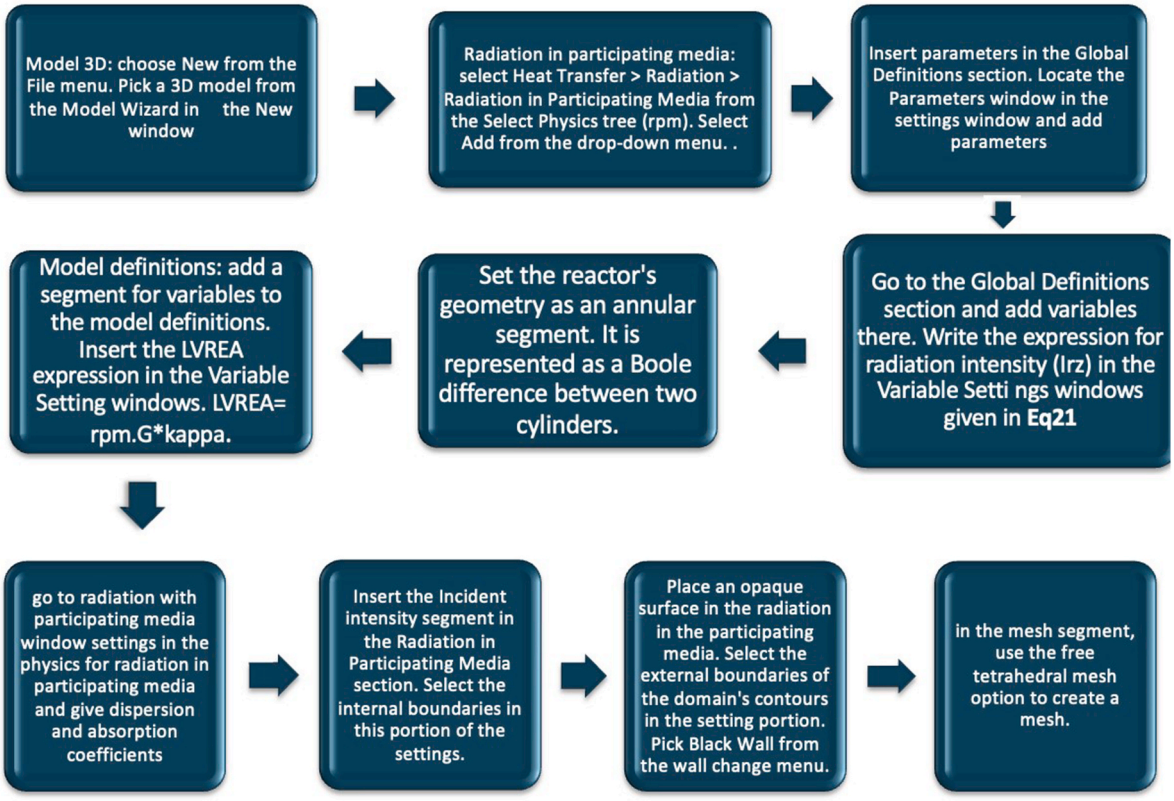

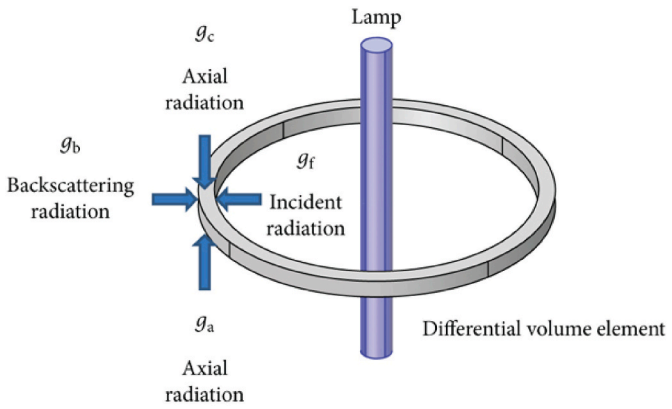

Fig. 2. Directions of the fluxes of photons in the four-flux model [6].

Despite being a simplified model, it retains core aspects of photoreactor radiation field modeling and has been successfully implemented at the solar pilot scale. The short computation times of the SFM are suitable for investigating the effects of operational parameters such as photocatalyst concentration, photoreactor measurements, and incident radiation. Table 2 shows the comparison between DOM and SFM.

Eq (27) gives the central equation of SFM:

$$\mathrm{LVRPA} = \mathrm{I}_0 \,/\, \lambda_{\omega\mathrm{corr}}\, \omega_{\mathrm{corr}} (1-\mathrm{r}) * \left[\left(\omega_{\mathrm{corr}} - 1 + \left(1 - \omega_{\mathrm{corr}}^2\right)^{-2} \right) \mathrm{e}^{-\mathrm{rp}/\lambda\omega\mathrm{corr}} + \gamma \left(\omega_{\mathrm{corr}} - 1 - \left(1 - \omega_{\mathrm{corr}}^2\right)^{-2} \right) \mathrm{e}^{-\mathrm{rp}/\lambda\omega\mathrm{corr}} \right] \tag{27}$$

Eg(27) For the CPCP and OMTP, however, a ray-tracing technique must be used following, since, in addition to incident radiation, the direction in which solar rays impact the photoreactor is critical.

The main screen of the PHOTOREAC GUI interface works as (1) The photoreactor panel, where the photoreactor configuration like CPCP, OMTP, and FPP was chosen.

(2) The system properties panel, where the input data for the simulation were introduced.
(3) The SFM model panel, where the SFM version for the simulation was selected.
(4) The SFM scattering phase function probabilities, according to the SFM variant that was selected.
(5) In the cross-section of the CPCP tunnel, the resulting LVRPA spatial distribution is plotted and the value is displayed.
(6) It is observed that the LVRPA is concentrated near the CPCP wall, and the centre of the tube shows shallow LVRPA values at a photocatalyst concentration of 0.2 g/L. Further, with the increase in catalyst, it shows higher LVREA values.

4. Results and discussions

4.1. Simulation

Sensitivity analysis helps to determine the optimum temperature and pressure at which there will be maximum output of the product. The results for methanol sensitivity analysis is shown in Fig. 3B. It is found that methanol selectivity in batch reactor occurs at T = 325 °C and P = 450 bar in Temp. and Pressure range of 200–400°C and 250–450 bar as compared to PFR in which it occurs at T = 250°C and P = 150 bar. The batch reactor shows a selectivity of methanol at around 1.78 which is lesser than the result given by PFR. PFR shows the selectivity of methanol as 6.56 mentioned in Aspen-Plus by Kamal I.M. Al-Malah [50].

Table 2
Comparison between DOM and SFM.

DOM	SFM
Models such as DOM and MC require a high computational effort for solving RTE in real reactor geometries.	SFM solves RTE in a simple algebraic way
The computational time for the RTE model evaluated is approximately 10 min which increases with finer mesh size.	The computational time in SFM is almost instantaneous
DOM provides the most accurate solution since the incident photos can also travel in the axial direction of the reactor	In SFM, the light is scattered in 6 cartesian directions leading to less accurate results as the scattering can occur in only six directions, this results in a high possibility for the particles close to the light source adsorbing the light onto the catalyst surface but not fully scattering the light.
DOM can be applied to any geometry and has no restrictions as compared to SFM.	SFM should be applied to geometries with lateral symmetry such as slabs, annular reactors, CPC, etc.

4.1.1. ASPEN HYSYS

4.1.1.1. ASPEN results. Here, there are in total 4 outlet streams as shown in Fig. 3A.

Inlet conditions and Outlet stream conditions are mentioned in Table 3 and Table 4 respectively.

4.1.1.2. Analysis. As per the simulations conducted, we observed after looking at the ratios of CO_2/H_2, CO/H_2, and CO_2/CO that the ratio of CO_2/H_2 is less than 1 which shows that H_2 is in excess in the reaction than CO_2. CO_2 acts as a limiting reagent. With the increase of the ratio, the methanol formation is decreased which shows that CO_2 is a stable molecule and is strongly bonded thus, decreasing the methanol formation. From the ratio of CO/H_2, we can see as we increase the ratio the methanol formation increases since CO is unstable and thus the bonds can be broken easily. So, high methanol formation depends on CO than H_2 but in both the reactions of CO_2 and CO hydrogenation H_2 is taken in excess. In the CO_2/CO ratio, we see the same trend as in CO_2/H_2 which says that CO_2 as compared to CO forms less amount of methanol

Fig. 4A, 4B and 4C: Rate of methanol formation for different ratios of CO_2 and H_2

4.1.2. PHOTOREAC

4.1.2.1. PHOTOREAC results. The photoreactors shown in the Fig. 5A, 5B and 5C consists of ten borosilicate tubes with radius R = 1 m and length L = 1 m providing a reaction volume of VR = 10 L. Model catalyst (TiO_2 P25 Evonik) concentration as 0.2 g/L. These results imply that CPC shows more VRPA(Volumetric Rate of Photon Absorption) as compared to FPP and OMTP. This activity is well-known in the literature and also proved that at high photocatalyst concentrations, photons are unable to penetrate deeply into the tube, and absorbed energy is localized along the tube's boundary wall [69].So, it is observed that the LVRPA is concentrated near the CPCP wall, and the centre of the tube shows shallow LVRPA values, with the increase in catalyst concentration. The reason is that CPCPs are equipped with reflectors which increase photon absorption. The ray-tracing technique was used jointly with the SFM to determine the direction of both the direct and diffuse solar photon fluxes and the spatial profile of the Local VolumetricRate of Photon Absorption (LVRPA) in the CPC reactor.

4.1.3. DWSIM

Fig. 6A and 6B shows the PFR flowsheet, conversion results, and graph of methanol conversion concerning reactor length. Here, we

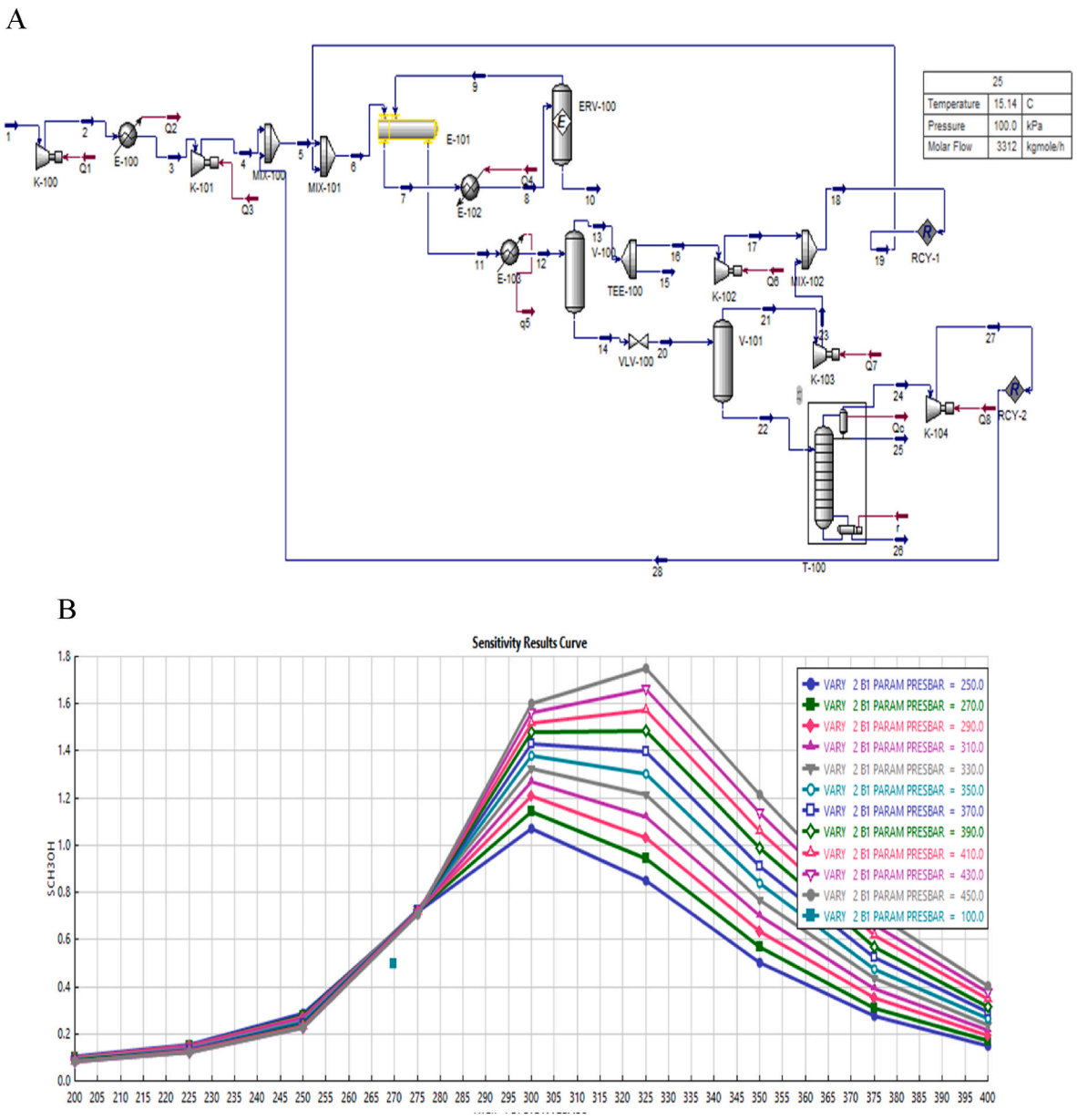

Fig. 3. A: Aspen Flow diagram, B: Aspen– Sensitivity result plot.

Table 3
Inlet stream conditions.

Name	1
Pressure [kPa]	5120
Temperature [C]	50
Mass Flow [kg/h]	128496
Std Ideal Liq Vol Flow [m^3/h]	371.489
Vapor/Phase Fraction	1
Molar Enthalpy [kJ/kgmole]	−53290.3
Utility Type	
Stream Price	
Stream Price Basis	Molar Flow
Cost Rate [Cost/s]	

Table 4
Outlet stream conditions.

Name	10	15	25	26
Pressure [kPa]	11000	11000	100	140
Temperature [C]	307.725	38	15.1387	109.246
Mass Flow [kg/h]	0	9187.49	105203	10639.4
Std Ideal Liq Vol Flow [m^3/h]	0	31.7392	131.819	10.6642
Vapor/Phase Fraction	0	1	0	0
Molar Enthalpy [kJ/kgmole]	−53347.6	−49854.6	−245090	−279594
Utility Type				
Stream Price				
Stream Price Basis	Molar Flow	Molar Flow	Molar Flow	Molar Flow
Cost Rate [Cost/s]				

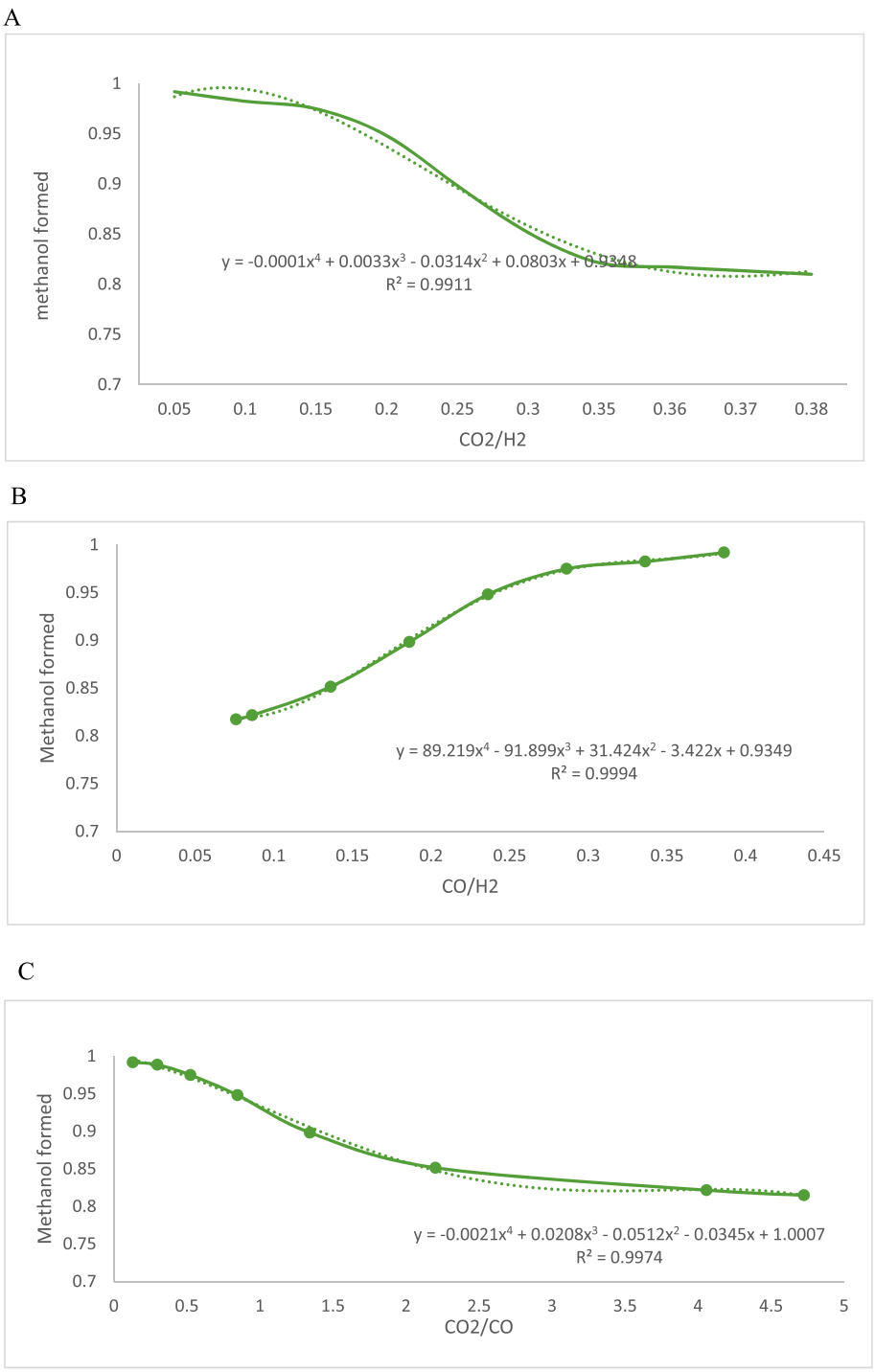

Fig. 4. A: Methanol formation for different CO_2/H_2 ratios, B: Methanol formation for different CO/H_2 ratios, C: Methanol formation for different CO_2/CO ratios.

observe that methanol gets formed in the middle of the reactor and remains constant with increasing temperature.

4.1.4. Design expert

Design Expert was used to fit the data simulated of a PFR reactor through DWSIM. squared value comes out to be 0.8756, as shown in Table 5 which implies a good fit of the data as shown in Fig. 7 and thus, the simulation of a PFR reactor is validated. Here the temperature was varied between 200 and 277 °C, pressure 30–50 bar, and catalyst weight 1500–2000 kg/m^3.

This implies R^2 implies that the overall mean may be a better predictor of the response than the current model. Adeq Precision measures the signal-to-noise ratio. A ratio greater than 4 is desirable. The model gives a ratio of 11.2238 which indicates an adequate signal.

By optimizing the data, we found temperature = 239.034°C, pressure = 40.3878 bar, and catalyst concentration of 1845.86 kg/m3 as the optimum operating parameters of the process concentration of 1845.86 kg/m^3 as the optimum operating parameters of the process which can be observed in Fig. 8.

4.1.5. COMSOL Multiphysics

Fig. 9 and Fig. 10 show radiation transport modeling of an Annular reactor in COMSOL wherein it shows the effect of catalyst concentration. It shows catalyst concentrations of 0.2 kg/m^3 and 0.4kg/m^3, wherein

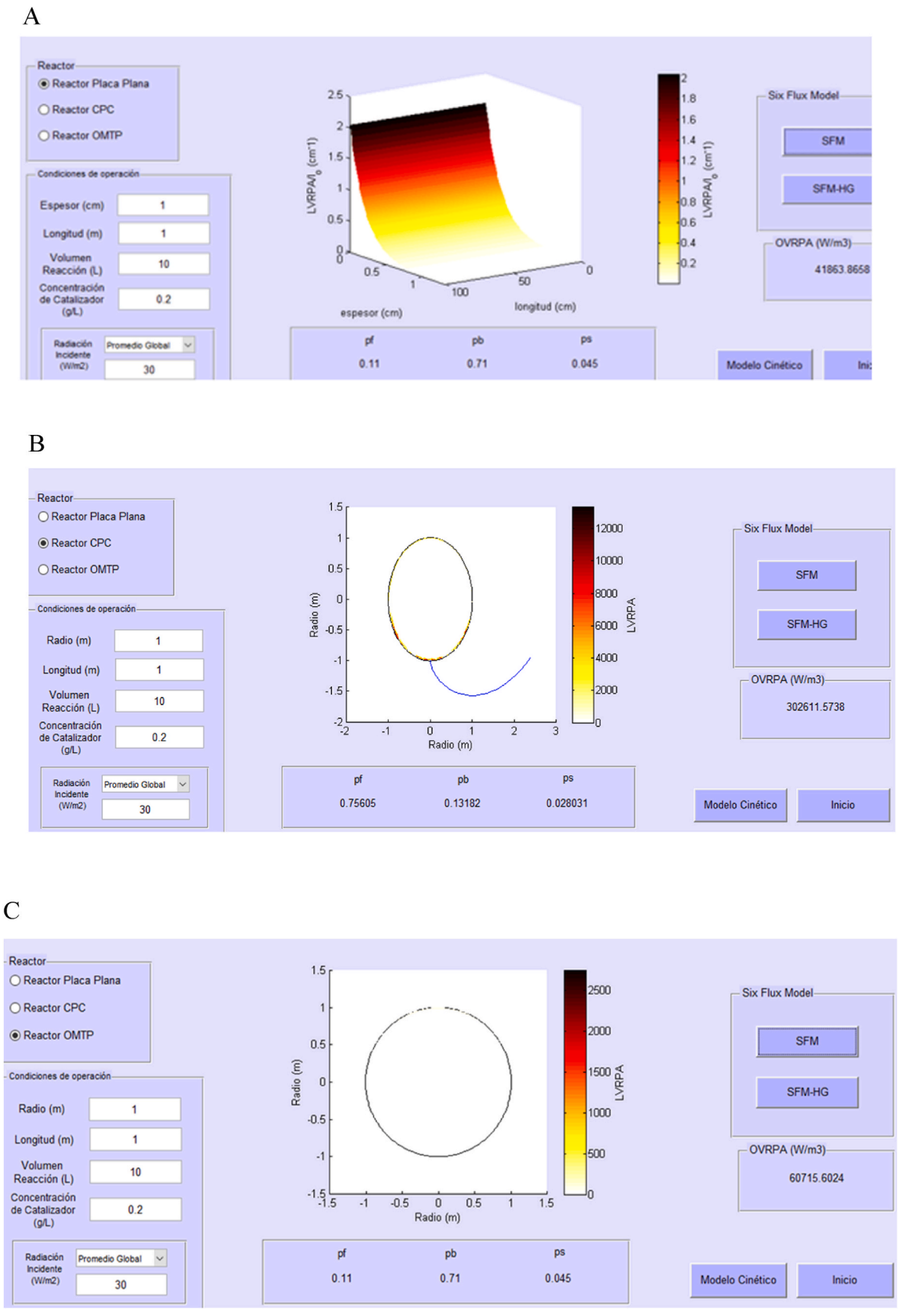

Fig. 5. A: Photoreactor with reactor plane, B: Photoreactor with CPC, C: Photoreactor with OMTP.

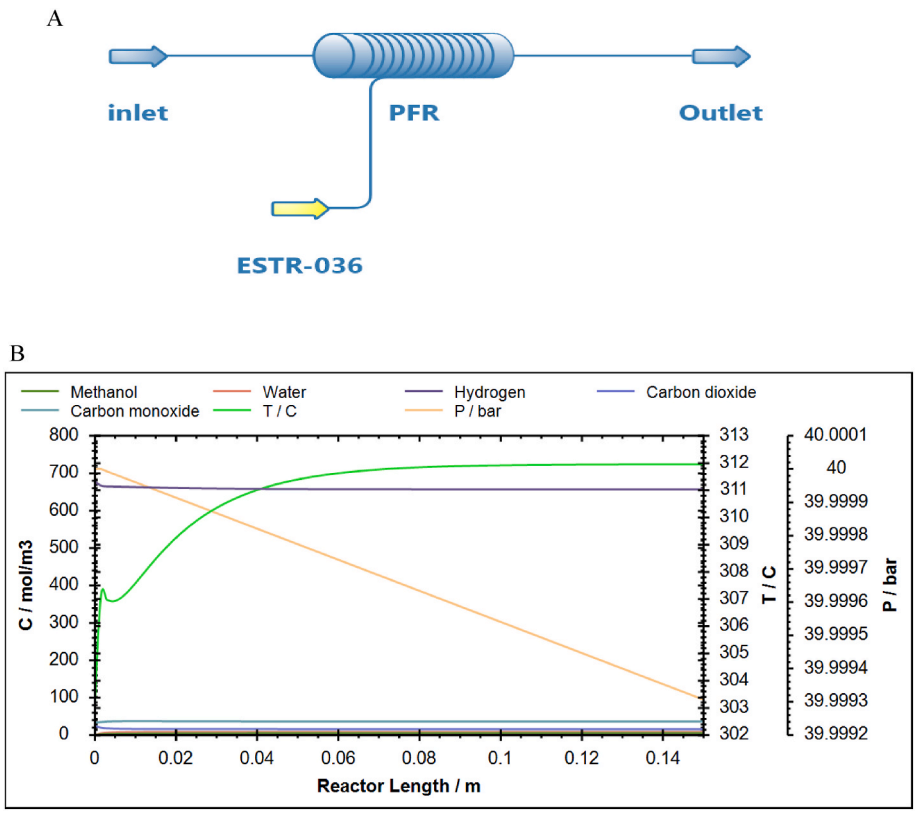

Fig. 6. A: DWSIM model, B: DWSIM simulation result.

Table 5
Fit statistics.

Std. Dev.	**0.2553**	R^2	**0.8756**
Mean	−4.37	**Adjusted R^2**	0.7636
C.V. %	5.84	**Predicted R^2**	−0.0238
		Adeq Precision	11.2238

LVREA values vary from 200 to 134W/m^3 and 395-285W/m^3 respectively. With the increase of catalyst concentration, the LVREA values increase. The particles close to the light source adsorb the light onto the catalyst surface but do not fully scatter the light to other catalyst particles. Therefore, the efficiency of the reactor becomes limited by the opacity, which reduces the number of particles being exposed to light penetration.

5. Conclusion

The escalating global energy demand, driven by rapid economic growth, has intensified the reliance on conventional fossil fuels, leading to elevated CO_2 concentrations and contributing to global warming. To combat this, innovative solutions like carbon capture and recycling have been proposed, converting CO_2 into versatile fuels like methanol using renewable H_2 sources. Methanol's versatility and industrial importance make it a compelling choice. Advanced mathematical tools, including MATLAB's ode23 and ode45 solvers, play a vital role in modelling complex differential equations essential for understanding chemical processes. Simulation platforms like DWSIM provide a comprehensive environment for experimentation, integrating thermodynamic models and unit operations. Design–Expert's role in optimization and robust parameter design is crucial for sustainable process development. Modelling techniques like the Discrete Ordinate Method deepen our understanding of radiative processes in photocatalysis. Despite challenges, these advancements are crucial for achieving cleaner and more sustainable energy practices.

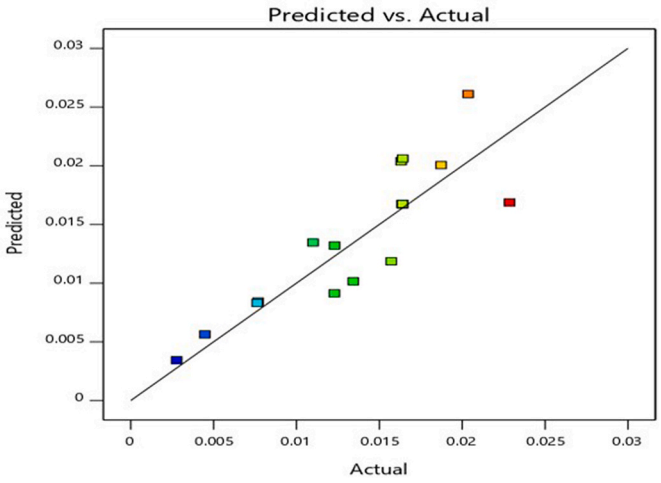

Fig. 7. Conversion variations concerning temperature, pressure, and catalyst concentration as factor.

1) Aspen HYSYS simulation was done for production of methanol to determine the feasibility on large scale at mass flowrate of 128496 kg/h where flue gases like H_2, N_2, CO, CO_2, CH_4, and H_2O were considered to have compositions of 0.6760, 0.0032, 0.0380, 0.2569, 0.0234, 0.0025, respectively. The ratio of CO_2/H_2, CO_2/CO, CO/H_2 was varied from 0.05 to 5 and methanol yield was calculated and was observed that lower the ratio of CO_2/H_2 and CO_2/CO the higher is

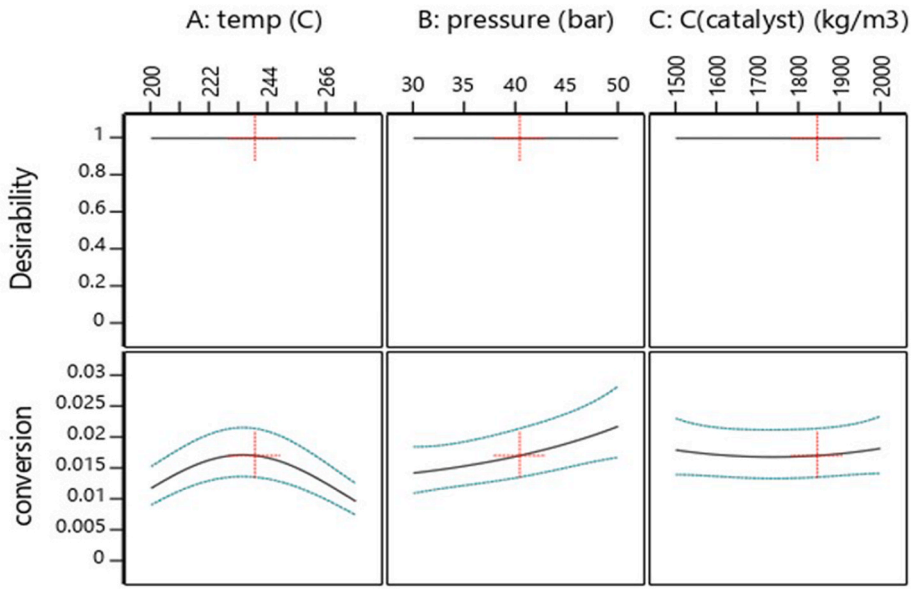

Fig. 8. The correlation between actual and predicted values.

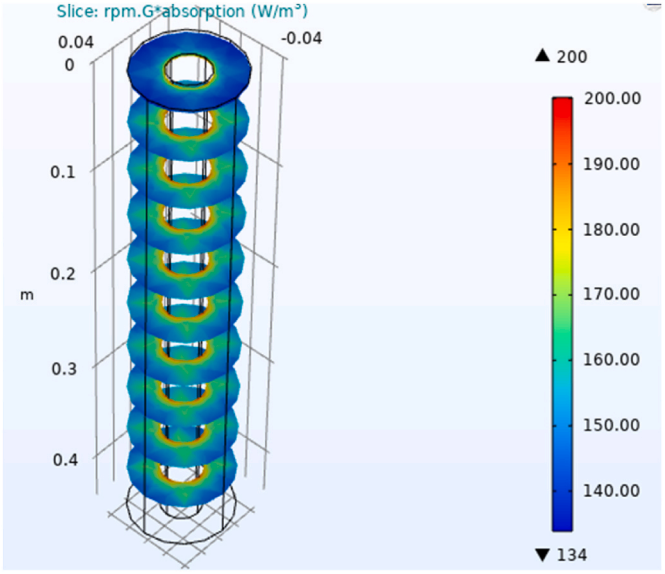

Fig. 9. DOM modelling of the annular reactor $C_{cat} = 0.2kg/m^3$:

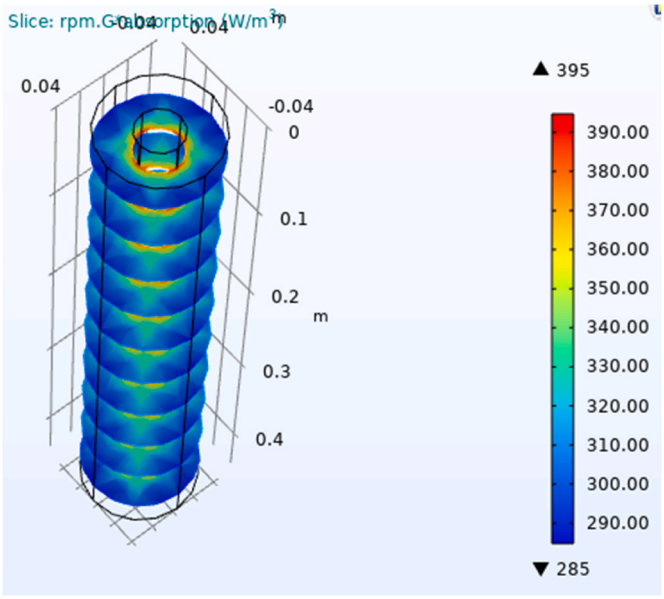

Fig. 10. DOM Modelling of the annular reactor $C_{cat} = 0.4kg/m^3$:

the yield of methanol and higher the ratio of CO/H_2 the lower is the yield of methanol.

2) PHOTOREAC simulation is done to observe the Volumetric Rate of Photon Absorption (VRPA) on various photoreactor like CPCP, FPP and OMTP. It was observed that CPCP has better photon adsorption on the walls of the reactor when compared to FPP and OMTP because of CPCP being equipped with reflectors to adsorb more photons.
3) Simulation of methanol producing plug flow reactor was done to determine that at what length does methanol conversion is more and to know the optimum length of reactor to get maximum conversion and it was observed that at 0.08 m the maximum conversion is achieved and is constant from there.
4) Design of experiments was used to determine the optimum temperature, pressure and catalyst concentration for plug flow reactor which was simulated in DWSIM software earlier.

After optimizing the parameter in DOE software, it was observed that at temperature of 239.034°C, pressure of 40.3878 bar and catalyst concentration of 1845.86 kg/m^3 maximum methanol conversion is achieved.

5) COMSOL simulation was performed to investigate the effect of light radiation w.r.t. catalyst concentration on LVREA value in an annular reactor. It was observed that the increase of catalyst concentration, the LVREA values increase and particles close to the light source adsorb the light onto the catalyst surface but do not fully scatter the light to other catalyst particles.

In the future prospect, the effect of intensity of light radiation on the catalyst behavior can be studied as well as the photocatalytic process can be further optimized to get more efficiency in methanol production.

CRediT authorship contribution statement

Ramyashree M.S.: Writing – review & editing, Investigation, Formal analysis, Data curation. **Aparajita Nandy:** Writing – original draft, Formal analysis, Data curation, Conceptualization. **Yash Rameshwar Bohari:** Writing – review & editing, Software, Formal analysis. **Mahika Pramodh:** Writing – review & editing, Formal analysis, Data curation. **S. Harish Kumar:** Writing – review & editing, Validation, Supervision. **S. Shanmuga Priya:** Writing – review & editing, Supervision, Project administration, Formal analysis. **K. Sudhakar:** Writing – review & editing, Validation, Supervision, Formal analysis.

Declaration of competing interest

The authors declare that they have no known competing financial interests or personal relationships that could have appeared to influence the work reported in this paper.

Data availability

No data was used for the research described in the article.

Acknowledgements

We extend our sincere gratitude to Manipal Academy of Higher Education, MAHE, Manipal, India, for the financial support of the research entitled “Carbon capture and conversion to methanol using the metal-organic framework as an adsorbent material” (Grant ID: 00000191/2019) and Vision Group on Science and Technology (VGST), Karnataka, India for the project fund entitled “Photocatalytic conversion of carbon dioxide to methanol using ZIF–8/$BiVO_4$/GO and rGO/CuO nanocomposites as an adsorbent material”(2020) (Ref No: VGST/RGS–F/GRD–918/2019–20/2020–21/198) and “Development of low cost and bio-based MOF for photocatalytic reduction of CO_2 to solar fuels"(Ref No: VGST/CESEM/GRD-1005/2021-22/425a)

References

[1] M.N. Hossain, J. Wen, A. Chen, Unique copper and reduced graphene oxide nanocomposite toward the efficient electrochemical reduction of carbon dioxide, Sci. Rep. 7 (2017), https://doi.org/10.1038/s41598-017-03601-3.

[2] D. Muliastri, D. Susanti, Widyastuti, Influence of composition grafit oxide, irradiation-time variation analyzes on reduced graphene oxide - copper oxide (rGO/CuO) composite toward photocatalytic conversion of CO2 to methanol, in: AIP Conf Proc, American Institute of Physics Inc., 2018, https://doi.org/10.1063/1.5054506.

[3] Y. Zhou, Z. Tian, Z. Zhao, Q. Liu, J. Kou, X. Chen, J. Gao, S. Yan, Z. Zou, High-yield synthesis of ultrathin and uniform Bi2WO6 square nanoplates Benefitting from photocatalytic reduction of CO2 into renewable hydrocarbon fuel under visible light, ACS Appl. Mater. Interfaces 3 (2011) 3594–3601, https://doi.org/10.1021/am2008147.

[4] W.-N. Wang, W.-J. An, B. Ramalingam, S. Mukherjee, D.M. Niedzwiedzki, S. Gangopadhyay, P. Biswas, Size and structure Matter: enhanced CO2 photoreduction efficiency by Size-Resolved Ultrafine Pt Nanoparticles on TiO2 single Crystals, J. Am. Chem. Soc. 134 (2012) 11276–11281, https://doi.org/10.1021/ja304075b.

[5] R. Acosta-Herazo, J. Monterroza-Romero, M.Á. Mueses, F. Machuca-Martínez, G. Li Puma, Coupling the Six Flux Absorption–Scattering Model to the Henyey–Greenstein scattering phase function: evaluation and optimization of radiation absorption in solar heterogeneous photoreactors, Chem. Eng. J. 302 (2016) 86–96, https://doi.org/10.1016/J.CEJ.2016.04.127.

[6] O. Alvarado-Rolon, R. Natividad, R. Romero, L. Hurtado, A. Ramírez-Serrano, Modelling and simulation of the radiant field in an annular heterogeneous photoreactor using a four-flux model, Int. J. Photoenergy 2018 (2018), https://doi.org/10.1155/2018/1678385.

[7] R.K. Derichter, T. Ming, S. Caillol, Fighting global warming by photocatalytic reduction of CO2 using giant photocatalytic reactors, Renew. Sustain. Energy Rev. 19 (2013) 82–106, https://doi.org/10.1016/J.RSER.2012.10.026.

[8] B. Tahir, M. Tahir, N.S. Amin, Performance analysis of monolith photoreactor for CO2 reduction with H2, Energy Convers. Manag. 90 (2015) 272–281, https://doi.org/10.1016/J.ENCONMAN.2014.11.018.

[9] D. Lu, M. Zhang, Z. Zhang, Q. Li, X. Wang, J. Yang, Self-organized vanadium and nitrogen co-doped titania nanotube arrays with enhanced photocatalytic reduction of CO2 into CH4, Nanoscale Res. Lett. 9 (2014) 1–9, https://doi.org/10.1186/1556-276X-9-272.

[10] K. Shu, B. Guan, J. Guo, X. Wu, Y. Chen, Z. Ma, J. Zhang, J. Chen, S. Yao, S. Bao, X. Jiang, L. Chen, H. Dang, Z. Guo, Z. Li, J. Hu, C. Yi, Z. Huang, The current Progresses and future perspectives of photoreactors and catalysts used in photocatalytic reduction of CO2, Ind. Eng. Chem. Res. 62 (2023) 15699–15732, https://doi.org/10.1021/acs.iecr.3c00728.

[11] J. Kothandaraman, A. Goeppert, M. Czaun, G.A. Olah, G.K. Surya Prakash, Conversion of CO2 from air into methanol using a Polyamine and a homogeneous Ruthenium catalyst, J. Am. Chem. Soc. 138 (2016) 778–781, https://doi.org/10.1021/jacs.5b12354.

[12] M.A. Hossen, H.M. Solayman, K.H. Leong, L.C. Sim, N. Yaacof, A. Abd Aziz, L. Wu, M.U. Monir, Recent progress in TiO2-Based photocatalysts for conversion of CO2 to hydrocarbon fuels: a systematic review, Results in Engineering 16 (2022), https://doi.org/10.1016/j.rineng.2022.100795.

[13] A.R.A. Astuti, W.H. Saputera, D. Ariono, I.G. Wenten, D. Sasongko, Membrane contactor-photocatalytic hybrid system for carbon dioxide capture and conversion to formic acid, Results in Engineering 22 (2024), https://doi.org/10.1016/j.rineng.2024.102085.

[14] L. Hamon, E. Jolimaître, G.D. Pirngruber, CO2 and CH4 separation by adsorption using Cu-BTC metal-organic framework, Ind. Eng. Chem. Res. 49 (2010) 7497–7503, https://doi.org/10.1021/ie902008g.

[15] B. Sakthivel, G. Nammalvar, Selective ammonia sensor based on copper oxide/reduced graphene oxide nanocomposite, J. Alloys Compd. 788 (2019) 422–428, https://doi.org/10.1016/J.JALLCOM.2019.02.245.

[16] J.-D. Xiao, H.-L. Jiang, Metal–organic frameworks for photocatalysis and Photothermal Catalysis, Acc. Chem. Res. 52 (2018) 356–366, https://doi.org/10.1021/acs.accounts.8b00521.

[17] Q. Zhang, L. Huang, S. Kang, C. Yin, Z. Ma, L. Cui, Y. Wang, CuO/Cu2O nanowire arrays grafted by reduced graphene oxide: synthesis, characterization, and application in photocatalytic reduction of CO2, RSC Adv. 7 (2017) 43642–43647, https://doi.org/10.1039/c7ra07310k.

[18] G. Leonzio, Mathematical modeling of a methanol reactor by using different kinetic models, J. Ind. Eng. Chem. 85 (2020) 130–140, https://doi.org/10.1016/J.JIEC.2020.01.033.

[19] G.H. Graaf, J.G.M. Winkelman, E.J. Stamhuis, A.A.C.M. Beenackers, Kinetics OF the three phase methanol synthesis. Tenth International Symposium on Chemical Reaction Engineering, 1988, pp. 2161–2168, https://doi.org/10.1016/B978-0-08-036969-3.50066-X.

[20] K.M. Vanden Bussche, G.F. Froment, A steady-state kinetic model for methanol synthesis and the water gas shift reaction on a commercial Cu/ZnO/Al2O3Catalyst, J. Catal. 161 (1996) 1–10, https://doi.org/10.1006/JCAT.1996.0156.

[21] F. Manenti, S. Cieri, M. Restelli, G. Bozzano, Dynamic modeling of the methanol synthesis fixed-bed reactor, Comput. Chem. Eng. 48 (2013) 325–334, https://doi.org/10.1016/J.COMPCHEMENG.2012.09.013.

[22] D. Rahman, Kinetic Modeling Of Methanol Synthesis From Carbon Monoxide, Carbon Dioxide, And Hydrogen Over A Cu/ZnO/Cr2O3 Catalyst, n.d. http://scholarworks.sjsu.edu/etd_theses.

[23] H.-W. Lim, M.-J. Park, S.-H. Kang, H.-J. Chae, J. Wook Bae, K.-W. Jun, Modeling of the kinetics for methanol synthesis using Cu/ZnO/Al2O3/ZrO2 catalyst: influence of carbon dioxide during hydrogenation, Ind. Eng. Chem. Res. 48 (2009) 10448–10455, https://doi.org/10.1021/ie901081f.

[24] R. Tamnitra, R. Jitwung, T. Puangpetch, W. Patthaveekongka, K. Leeheng, Kinetic Modeling and Simulation of Bio-Methanol Process from Biogas by Using Aspen Plus, MATEC Web of Conferences, EDP Sciences, 2018, https://doi.org/10.1051/matecconf/201819203030.

[25] N.J. Azhari, D. Erika, S. Mardiana, T. Ilmi, M.L. Gunawan, I.G.B.N. Makertihartha, G.T.M. Kadja, Methanol synthesis from CO2: a mechanistic overview, Results in Engineering 16 (2022), https://doi.org/10.1016/j.rineng.2022.100711.

[26] G. Leonzio, E. Zondervan, P.U. Foscolo, Methanol production by CO2 hydrogenation: analysis and simulation of reactor performance, Int. J. Hydrogen Energy 44 (2019) 7915–7933, https://doi.org/10.1016/J.IJHYDENE.2019.02.056.

[27] S. Sharifian, M. Miltner, M. Harasek, Thermodynamic and kinetic based simulation approach to CO2 and CO methane hydrogenation, Chem Eng Trans 52 (2016) 565–570, https://doi.org/10.3303/CET1652095.

[28] R. Tamnitra, R. Jitwung, T. Puangpetch, W. Patthaveekongka, K. Leeheng, Kinetic Modeling and Simulation of Bio-Methanol Process from Biogas by Using Aspen Plus, MATEC Web of Conferences, EDP Sciences, 2018, https://doi.org/10.1051/matecconf/201819203030.

[29] W.-N. Wang, J. Soulis, Y.J. Yang, P. Biswas, Comparison of CO2 photoreduction systems: a review, Aerosol Air Qual. Res. 14 (2014) 533–549, https://doi.org/10.4209/aaqr.2013.09.0283.

[30] S. Ali, M.C. Flores, A. Razzaq, S. Sorcar, C.B. Hiragond, H.R. Kim, Y.H. Park, Y. Hwang, H.S. Kim, H. Kim, E.H. Gong, J. Lee, D. Kim, S. Il In, Gas phase photocatalytic CO2 reduction, “a brief overview for benchmarking,”, Catalysts 9 (2019) https://doi.org/10.3390/catal9090727.

[31] S.E.M. Elhenawy, M. Khraisheh, F. Almomani, G. Walker, Metal-organic frameworks as a platform for CO2 capture and chemical processes: adsorption, membrane separation, catalytic-conversion, and electrochemical reduction of CO2, Catalysts 10 (2020) 1–33, https://doi.org/10.3390/catal10111293.

[32] R. Acosta-Herazo, B. Cañaveral-Velásquez, K. Pérez-Giraldo, M.A. Mueses, M. H. Pinzón-Cárdenas, F. Machuca-Martínez, A MATLAB-based application for modeling and simulation of solar Slurry photocatalytic reactors for environmental applications, Water (Switzerland) 12 (2020), https://doi.org/10.3390/W12082196.

[33] V.K. Pareek, M.P. Brungs, A.A. Adesina, Continuous process for photodegradation of industrial bayer liquor, Ind. Eng. Chem. Res. 40 (2001) 5120–5125, https://doi.org/10.1021/ie0010058.
[34] V.K. Pareek, S.J. Cox, M.P. Brungs, B. Young, A.A. Adesina, Computational fluid dynamic (CFD) simulation of a pilot-scale annular bubble column photocatalytic reactor, Chem. Eng. Sci. 58 (2003) 859–865, https://doi.org/10.1016/S0009-2509(02)00617-6.
[35] Mathematical model of a flat plate photocatalytic reactor irradiated by solar light, Czasopismo Techniczne (2017), https://doi.org/10.4467/2353737xct.17.191.7420.
[36] M. Janczarek, E. Kowalska, Computer simulations of photocatalytic reactors, Catalysts 11 (2021) 1–15, https://doi.org/10.3390/catal11020198.
[37] M. Marečić, F. Jović, V. Kosar, V. Tomašic, Modelling of an annular photocatalytic reactor, React. Kinet. Mech. Catal. 103 (2011) 19–29, https://doi.org/10.1007/s11144-011-0299-y.
[38] W.B. Ye, M. Arıcı, 3D validation, 2D feasibility, corrected and developed correlations for pure solid-gallium phase change modeling by enthalpy-porosity methodology, Int. Commun. Heat Mass Tran. 144 (2023) 106780, https://doi.org/10.1016/J.ICHEATMASSTRANSFER.2023.106780.
[39] W.B. Ye, M. Arıcı, Exploring mushy zone constant in enthalpy-porosity methodology for accurate modeling convection-diffusion solid-liquid phase change of calcium chloride hexahydrate, Int. Commun. Heat Mass Tran. 152 (2024) 107294, https://doi.org/10.1016/J.ICHEATMASSTRANSFER.2024.107294.
[40] W.B. Ye, M. Arıcı, False diffusion, asymmetrical interface, and equilibrious state for pure solid-gallium phase change modeling by enthalpy-porosity methodology, Int. Commun. Heat Mass Tran. 144 (2023) 106746, https://doi.org/10.1016/J.ICHEATMASSTRANSFER.2023.106746.
[41] W.B. Ye, M. Arıcı, Redefined interface error, 2D verification and validation for pure solid-gallium phase change modeling by enthalpy-porosity methodology, Int. Commun. Heat Mass Tran. 147 (2023) 106952, https://doi.org/10.1016/J.ICHEATMASSTRANSFER.2023.106952.
[42] J. Moreno-SanSegundo, C. Casado, J. Marugán, Enhanced numerical simulation of photocatalytic reactors with an improved solver for the radiative transfer equation, Chem. Eng. J. 388 (2020) 124183, https://doi.org/10.1016/J.CEJ.2020.124183.
[43] N.S. Topare, S.J. Raut, S.J. Attar, 3D model design and simulation OF photocatalytic reactor for degradation OF DYES using SOLIDWORKS, Software (2012). www.sadgurupublications.com.
[44] J. Wang, B. Deng, J. Gao, H. Cao, Numerical simulation of radiation distribution in a slurry reactor: the effect of distribution of catalyst particles, Chem. Eng. J. 357 (2019) 169–179, https://doi.org/10.1016/J.CEJ.2018.09.126.
[45] S. Gai, J. Yu, H. Yu, J. Eagle, H. Zhao, J. Lucas, E. Doroodchi, B. Moghtaderi, Process simulation of a near-zero-carbon-emission power plant using CO2 as the renewable energy storage medium, Int. J. Greenh. Gas Control 47 (2016) 240–249, https://doi.org/10.1016/J.IJGGC.2016.02.001.
[46] M.K.G.P.N. Ghasemian, N. Ghasemian, M. Kalbasi, G. Pazuki, Experimental study and mathematical modeling of solubility of CO2 in water: application of artificial neural network and Genetic Algorithm, J. Dispersion Sci. Technol. 34 (2013) 347–355, n.d.
[47] B.L. Salvi, S. Jindal, Recent developments and challenges ahead in carbon capture and sequestration technologies, SN Appl. Sci. 1 (2019), https://doi.org/10.1007/s42452-019-0909-2.
[48] R. Guil-López, N. Mota, J. Llorente, E. Millán, B. Pawelec, J.L.G. Fierro, R. M. Navarro, Methanol synthesis from CO2: a review of the latest developments in heterogeneous Catalysis, Materials 12 (2019) 3902, https://doi.org/10.3390/ma12233902.
[49] C. Casado, J. Marugán, R. Timmers, M. Muñoz, R. van Grieken, Comprehensive multiphysics modeling of photocatalytic processes by computational fluid dynamics based on intrinsic kinetic parameters determined in a differential photoreactor, Chem. Eng. J. 310 (2017) 368–380, https://doi.org/10.1016/J.CEJ.2016.07.081.
[50] R. Schefflan, Teach Yourself the Basics of Aspen Plus, Second, John Wiley & Sons, 2016 n.d.
[51] A. Tripodi, M. Compagnoni, R. Martinazzo, G. Ramis, I. Rossetti, Process simulation for the design and scale up of heterogeneous catalytic process: kinetic modelling issues, Catalysts 7 (2017), https://doi.org/10.3390/catal7050159.
[52] K.I.M. AL-MALAH, No Title, n.D, (n.d.).
[53] S. Perry, R.H. Perry, D. W. Green, J.O. Maloney, Chemical Engineers' Handbook, Seventh, Mc Grawhill. 2008 n.d.
[54] K. Tangsriwong, P. Lapchit, T. Kittijungjit, T. Klamrassamee, Y. Sukjai, Y. Laoonual, Modeling of chemical processes using commercial and open-source software: a comparison between Aspen plus and DWSIM, in: IOP Conf Ser Earth Environ Sci, Institute of Physics Publishing, 2020, https://doi.org/10.1088/1755-1315/463/1/012057.
[55] S.S.O. Silva, M.R. Nascimento, R.J.P. Lima, F.M.T. Luna, C.L. Cavalcante Júnior, Experimental and simulation studies for purification and Etherification of Glycerol from the biodiesel industry, AppliedChem 3 (2023) 492–508, https://doi.org/10.3390/appliedchem3040031.
[56] The Minerals Metals & Materials Society (TMS), TMS 2023 152nd Annual Meeting & Exhibition Supplemental Proceedings, 2023. , (n.d.).
[57] M.A. Mohd Ariff, N.A. Mohd Nasir, Z. Abdul Rashid, F.S. Rohman, Optimization of an industrial methanol reactor using aspen plus simulator and design expert, ESTEEM Acad. J. 19 (2023) 37–50, n.d.
[58] A. Manuscript, Catal. Sci. Technol., (n.d.)., (n.d.).
[59] R. Binjhade, R. Mondal, S. Mondal, Continuous photocatalytic reactor: critical review on the design and performance, J. Environ. Chem. Eng. 10 (2022) 107746, https://doi.org/10.1016/J.JECE.2022.107746.
[60] G.L. Morrison, Solar collectors, Sol. Energy State Art (2013) 145–222, n.d.
[61] K.P. Sundar, S. Kanmani, Progression of Photocatalytic reactors and it's comparison: a Review, Chem. Eng. Res. Des. 154 (2020) 135–150, https://doi.org/10.1016/J.CHERD.2019.11.035.
[62] T.A. Egerton, Uv-absorption-the primary process in photocatalysis and some practical consequences, Molecules 19 (2014) 18192–18214, https://doi.org/10.3390/molecules191118192.
[63] T. Nottingham, Mutsee Termtanun, Photocatalytic Degradation of Pesticides Using TiO2 Nanoparticles, PhD thesis, University of Nottingham . PHOTOCATALYTIC DEGRADATION OF PESTICIDES USING TIO2 NANOPARTICLES BY PHILOSOPHY NOVEMBER 2013, 2013 (2013) 239., (n.d.).
[64] S.C. Mishra, H.K. Roy, N. Misra, Discrete ordinate method with a new and a simple quadrature scheme, J. Quant. Spectrosc. Radiat. Transf. 101 (2006) 249–262, https://doi.org/10.1016/J.JQSRT.2005.11.018.
[65] P.S. Roy, R. Amin, Aspen-HYSYS Simulation of Natural Gas Processing Plant, 2011.
[66] M. Hoorfar, Y. Alcheikhhamdon, B. Chen, A novel tool for the modeling, simulation and costing of membrane based gas separation processes using Aspen HYSYS: optimization of the CO2/CH4 separation process, Comput. Chem. Eng. 117 (2018) 11–24, https://doi.org/10.1016/J.COMPCHEMENG.2018.05.013.
[67] W.H. Saputera, J.J. Pranata, R. Jonatan, P. Widiatmoko, D. Sasongko, Photocatalytic simulation of Phenol waste degradation using titanium dioxide (TiO2) P25-based photocatalysts, Journal of Engineering and Technological Sciences 55 (2023) 419–433, https://doi.org/10.5614/j.eng.technol.sci.2023.55.4.6.
[68] S. Chantasiriwan, Simulation and optimization of vapor absorption Refrigeration system using DWSIM, Chem Eng Trans 100 (2023) 613–618, https://doi.org/10.3303/CET23100103.
[69] M. Vajdi, F. Sadegh Moghanlou, F. Sharifianjazi, M. Shahedi Asl, M. Shokouhimehr, A review on the Comsol Multiphysics studies of heat transfer in advanced ceramics, Journal of Composites and Compounds 2 (2020) 35–44, https://doi.org/10.29252/jcc.2.1.5.